A new green protocol for the identification of microplastics and microfibers in marine sediments, a case study from the Vesuvian Coast, Southern Italy

Journal of Hazardous Materials 477 (2024) 135272

Contents lists available at ScienceDirect

Journal of Hazardous Materials

journal homepage: www.elsevier.com/locate/jhazmat

Research Article

A new green protocol for the identification of microplastics and microfibers in marine sediments, a case study from the Vesuvian Coast, Southern Italy

Manuela Rossi [a,b,*], Alessandro Vergara [c], Fiore Capozzi [d], Simonetta Giordano [d], Valeria Spagnuolo [d], Romualdo Troisi [c], Vincenzo Vedi [a], Filippo Ambrosi de Magistris [e], Noemi Fiaschini [f], Tonia Tommasi [g], Marco Guida [d], Mariarca D'Aniello [a,h], Carlo Donadio [a,i]

[a] Department of Earth Sciences, Environment and Resources, University of Napoli Federico II, Napoli, Italy
[b] Institute of Crystallography, CNR, Bari, Italy
[c] Department of Chemical Sciences, University of Napoli Federico II, Napoli, Italy
[d] Department of Biology, University of Napoli Federico II, Napoli, Italy
[e] Optical Division Carl Zeiss, Italy
[f] Nanofaber Srl, Via Anguillarese, 301, Roma 00123, Italy
[g] Department of Applied Science and Technology, Politecnico di Torino, Torino, Italy
[h] National Institute for Astrophysics, INAF-OAC, Napoli, Italy
[i] Stazione Zoologica Anton Dohrn, Napoli, Italy

HIGHLIGHTS

- Microplastics and microfibers morphological characterization in marine sediments.
- New experimental protocol with optical microscopy without sample pretreatments.
- Optical microscopy on live image and photograph analysis.
- Sediments from the berm and the shoreline of Vesuvian Coast.
- Accumulation processes of microparticles and pollutant sources.

GRAPHICAL ABSTRACT

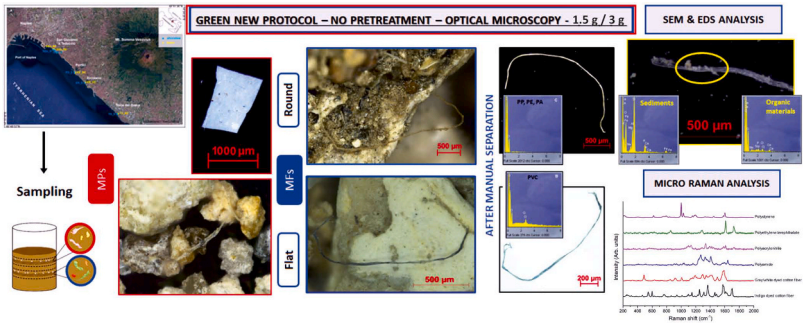

ARTICLE INFO

Keywords:
Microplastics and microfibers
Marine environment
Experimental protocol
Optical microscopy
Micro Raman
Vesuvian Coast

ABSTRACT

Microplastics (MP; 1 μm–5 mm) and microfibers (MF; thin, elongated particles with a high-length-to-width ratio) have become a major global environmental issue due to their ubiquity in the oceans and possess complex physicochemical properties that vary their mobility, bioavailability, and toxicity toward organisms and interactions with their surrounding pollutants. Nonetheless, a reliable methodology that would facilitate and automate the monitoring of MP is still lacking. Intending to select practical and standardized methods and considering the challenges in MPs detection, a new analysis protocol based on optical microscopy for the counting and morphological analysis of the particles has been developed. This method overcomes some issues related to the lack of practicality and standardization of the others currently applied, and does not involve sieving, washing, heating, or density separation and digestion processes. Our method is green and requires a

* Corresponding Author at: Department of Earth Sciences, Environment and Resources, University of Napoli Federico II, Napoli, Italy.
E-mail address: manuela.rossi@unina.it (M. Rossi).

https://doi.org/10.1016/j.jhazmat.2024.135272
Received 22 May 2024; Received in revised form 11 July 2024; Accepted 19 July 2024
Available online 25 July 2024

minimum quantity of sediment, i.e., 1.5 g, and shortened timeframes. Future research efforts may need to develop and implement new analytical tools and combinations of technologies to complement respective detection limitations and yield reliable characterization of both MFs and MPs. We tested our protocol to study, for the first time, both marine and land sediment in the Vesuvian area of the Gulf of Naples (Italy).

1. Introduction

Plastic litter is a ubiquitous pollutant increasingly detected in various environments. Due to their broad applications, massive amounts of plastic-containing products end up in solid waste and enter waterways [1,2]. This fact poses potential risks to human health and ecological systems such as aquatic organisms or animals if ingested directly or indirectly through the food chain [3,4]. Plastic waste discharged into the environment undergoes alteration processes and interactions with the environmental matrix or organisms such as bacteria and pollutants [5]. Plastics then undergo processes of "fragmentation or deconstruction" into smaller pieces like microplastics (MPs), which range in size from 1 μm to 5 mm, or microfibers (MFs), defined as thin, elongated MPs with a high length-to-width ratio between 3:1 and 5:1 [6-9].

Fragmentation and deconstruction refer to forming or releasing smaller particles from the larger, original object. The physicochemical properties of MPs and MFs (e.g., shape, size, concentrations, surface charge, hydrophobicity) affect transformation, interaction with the hosting environment, fate in water systems, and their bioavailability for aquatic organisms [10,11].

As for MFs, in 20 years, the world production of textile fibers has doubled, and the most recent synthetic fabrics are responsible for most of this growth. This trend is expected to continue to increase, raising severe concerns due to their long degradation time [12].

Accurate acquisition of physical and chemical properties and the use of several advanced microscopic and spectroscopic techniques are essential for understanding the behaviour and bioavailability of MPs and MFs, which ultimately delivers new insight into the prevention and mitigation of environmental risks [13]. Microplastics comprise a range of constituent polymers, according to their constituent base monomers, and exhibit a range of morphologies, physical, and chemical properties. Regarding microfibers, detailed studies on their physicochemical properties are lacking, especially when it comes to morphological aspects. Some physical properties are used to highlight their presence and separate them from the matrices in which they are found.

The detection of microplastic particles usually involves the following steps: 1) extraction from the matrix; 2) isolation and quantification; 3) characterization and identification [14]. The separation methods are classified into active and passive sorting techniques [15]. Density-based separation method is the most credible and commonly used method for separating microplastics from sediment or sand [15].

The currently existing protocols for separating microplastics from sediments are based on density separation and digestion processes. Density-based separation utilizes solutions with high specific gravity and is amongst the most applied methods used to separate plastic from heavier sample matrices, such as sediments [16-21]. Sequential density extraction procedures may also be used to isolate particles based on their behavior in different aqueous media, for example, freshwater and saturated salt (NaCl). Denser liquids, such as NaI, are required to separate more dense particles. Limitations of density separation include the inability of salts to extract the densest polymers, from sediments and the influence of biofilms and other fouling material on net polymer density [8].

A digestion process is commonly associated with gravity separation to remove non-plastic organic material. A commonly applied digestion technique for removing organic material from environmental matrices is oxidation using H_2O_2, acidic (HCl and HNO_3), and alkaline (KOH and NaOH) digestion procedures. These methodologies have been questioned because it has been demonstrated that they may alter the surface of MPs particles, leading in some cases even to their complete degradation (Harley et al., 2018; [18]). A potential alternative is the use of Fenton's reagent. Ferrous sulphate is commonly used as an iron catalyst component, and the composition of sewage sludge may reduce the efficacy of organic matter removal. Less damaging processes, such as enzymatic digestion, can be a suitable alternative but can also be very time-consuming and expensive ([22,23,8] and references therein).

It should also be noted that existing protocols involve the use of temperatures up to 110 °C for the preparation of sediment samples [24] and up to 60 °C during the digestion process [17]. The temperature associated with the materials used in different protocols could cause polymer degradation [17]. The protocol described in Ferrante et al. [25] involves the use of a minimal sample quantity for the extraction of MPs with a density greater than 1 g/cm^3 from various environmental matrices including sediments. In the description of this protocol, sample pretreatment includes the use of nitric acid, dichloromethane, and acetonitrile, as well as vortexing and centrifugation. Although this protocol involves using a minimal sample quantity, applying it to sediment samples could potentially cause chemical and physical damage to the MPs and MFs [26].

The various protocols used for MPs separation and organic matter removal from their surface entail drawbacks that make them unsuitable for independent use [8]. Furthermore, these protocols entail the loss of some information (incorrect counting and morphological characterization) that can lead to misinterpretation regarding their origin and potential environmental impacts [27,28,8,29]; (Harley et al., 2018). This is particularly true for smaller microparticles like microfibers [26,30], more abundant than microplastics in sediments (Harris et al., 2020).

In recent years, numerous studies have been conducted to expedite the characterization, both morphological and chemical, of MPs, using various spectroscopic techniques (NIR-HIS, FTIR, ATR), advanced image data management software for optical microscopy, and sometimes combined techniques [15]. In Goyetche et al. [14], the combination of suitable machine learning classification models and NIR-HSI applied under appropriate circumstances, on sediments, has the potential to be a valuable addition to microplastic monitoring protocols, given its adaptability, ability to gather data over large areas in a short time, and low sample preparation requirements. However, this method also presents challenges in data acquisition and processing. One of the main challenges arises from the fact that the chemical classification and recognition of microplastics are based on spectral libraries of pure polymers, while MPs found in the environment are not pure. Furthermore, the presence of sediment fragments (inorganic materials) on the surface of MPs, their irregular surfaces, and the small dimensions influence detection using NIR radiation and can generate spectral artifacts. Finally, the mineralogical composition of the sands in which MPs are to be studied should not be underestimated, as this could significantly complicate the implementation of the protocol by Goyetche et al. [14]. Therefore, caution is necessary when dealing with complex mineralogical compositions of sands and their high and variable spatial heterogeneity. It is worth noting that this protocol cannot be applied to the study of MFs, as highlighted by the authors themselves. The method presented in Peiponen et al. [31] involves observations in stereomicroscopy, in transmitted light. In this protocol, the sample consisting exclusively of MPs and MFs must be diluted in water. Therefore, additional equipment is required to handle the sample dilution and pump the solution into a flow cell, where the transmitted light image data is collected. Subsequently, this data is processed and converted into a quantitative one. Peiponen et al. [31] recommend using this method for

the study of MPs and MFs in water, but if samples from other matrices undergo separation pretreatments, it could be applied to MPs and MFs from different environments as well. Ocampo et al. [32] describe the morphology of MPs isolated from a cosmetic cream using a self-written Python-based script, which processes and analyzes image data. The sample involves pretreatment of the MPs, which are isolated and thoroughly cleaned. Ocampo et al. [32] define this protocol as not applicable to the characterization of MFs. This method describes the MPs shape and degree of surface roughness and smoothness and could be applied to MPs from any environmental matrix. MPs must be cleaned and separated from each other. Actually, the presence of microparticles unrelated to MPs, whether organic (e.g., algae colonies) or inorganic (small fragments of minerals and rocks), can lead to an erroneous description of the shape and of surface roughness and smoothness degree. Additionally, MPs must not be present in aggregates, for the aforementioned reasons. Abaroa-Pérez et al., [33] evaluate and quantify the degradation state of marine microplastic polyethylene pellets at different aging stages using Yellowness Index (YI) determination and FTIR spectrum analysis.

This work aims to develop an improved protocol for the separation, counting, and morphological characterization of MPs, focusing particularly on MFs, based on optical microscopy observation without any sample pre-treatment. We were inspired by existing methodologies for the characterization of MPs in water (recognition, counting, characterization, e.g., protocols outlined by [34,35,29]), herein extended to MPs in marine sediments, without a gravity separation and digestion process. In this way, MPs and MFs undergo no alteration due to digestion processes, as highlighted by Lusher et al. [8] and Harris [28]. Additionally, due to the presence of encrustations and sediment granules on their surface, they are not removed during gravity separation processes, and MFs are not at risk of dissolution during digestion processes.

The analytical procedures for the characterization of MPs and MFs are applied on sediments from the berm and the shoreline located southeast of the Gulf of Naples, the coastal sector between the ports of San Giovanni a Teduccio (NW) and Torre del Greco (SE) (10 samples). Differently from other methodologies and techniques, this multidisciplinary study on MPs and MFs in sediments is based, for the first time on (1) sampling along beach through the morphological criterion and related facing seawater, (2) investigations using stereomicroscopy for counting and morphological analysis, (3) SEM for detailed morphological data, (4) EDS and Micro-Raman spectroscopy for chemical investigations, (5) granulometric and grain morphoscopic analyses, the results of which are compared each other.

2. Materials and methodS

2.1. Sampling site

The coastal sector between the ports of Torre del Greco and San Giovanni a Teduccio (NW) is part of the Vesuvian Coast, which extends for about 16 km up to the port of Torre Annunziata (SE) and represents the southern termination of the western side of the volcanic edifice of Mt. Somma-Vesuvius (a detailed description of the sampling site can be found in the Supplementary Materials).

2.2. Sampling

Samples sediments (SGa_S, SGa_BE, SGb_S, SGb_BE, PO_S, PO_BE, ER_S, ER_BE, TG_S, TG_BE) were collected from 4 urban beaches [36] on the Vesuvius coast: San Giovanni a Teduccio (SG), Portici (PO), Ercolano (ER) and Torre del Greco (TG). Two samples were taken for each site, one on the ordinary or storm berm (BE) and another on the shoreline (S) about 10 m away, in May 2021 (Fig. 1, Table 1). A double sampling of shoreline and storm berm was carried out on the beach of San Giovanni a Teduccio due to the larger dimensions of this beach (sampling sites a and b). Samples for MPs and MFs analysis were 1 kg in weight and were collected by a steel shovel and packed with an aluminum tray to avoid MPs contaminations.

2.3. Sedimentological analysis

The sedimentological analysis consisted of the determination of granulometry and morphoscopic features of the surfaces of quartz and silicate (K-felspar and Na-plagioclase) granules [37-39]. In particular, after preparation and washing with a vacuum pump, samples were dried

Fig. 1. Location and code of beach samples collected from the shoreline (S, cyano) and berm (BE, yellow) of the Vesuvian Coast: SGa, and b, San Giovanni a Teduccio, Spiaggia delle Industrie; PO, Portici, Spiaggia delle Mortelle; ER, Ercolano, Spiaggia La Favorita; TG, Torre del Greco, Miramare. The geographic coordinate system is WGS84 (Google Earth Pro, 2024 mod.). For more details, refer to Tables 2.

Table 1
List of the land samples, location of sampling points, latitude, longitude, type.

n.	ID_sample	Site	Latitude	Longitude	Type
1	SGa-S	Spiaggia delle Industrie	40°49'43.0"	14°18'36.8"	Shoreline
2	SGa-BE	Spiaggia delle Industrie	40°49'43.0"	14°18'37.8"	Berm
3	SGb-S	Spiaggia delle Industrie	40°49'40.9"	14°18'40.0"	Shoreline
4	SGb-BE	Spiaggia delle Industrie	40°49'41.1"	14°18'40.3"	Berm
5	PO-S	Le Mortelle	40°48'23.3"	14°20'08.6"	Shoreline
6	PO-BE	Le Mortelle	40°48'23.1"	14°20'08.9"	Berm
7	ER-S	La Favorita	40°47'48.8"	14°20'53.3"	Shoreline
8	ER-BE	La Favorita	40°47'48.7"	14°20'53.8"	Berm
9	TG-S	Miramare	40°45'56.8''	14°23'20.3''	Shoreline
10	TG-BE	Miramare	40°45'56.7''	14°23'20.7''	Berm

Number and localization of sampling stations of beaches from northwest to southeast.

in an oven at 40 °C for 72 h, mechanically quartered, weighed with the electronic scale OHAUS PR423 with a resolution of 0.001 g, and subjected to dry sieving through an ASTM series of stacked sieves, with 1/2 ϕ class interval from 8000 down to 63 μm, in a Ro-Tap mechanical sieve shaker for 15'. Fractions < 63 to 2 μm were not determined, as they resulted always in < 1 % of the total net weight of the sample, well below the 5 % granulometric threshold. For each sample, histograms, triangular diagrams, and cumulative frequency curves were plotted by the software Gradistat v.9 [40]. Statistical parameters as mean size (Mz), mode (Mo), median (D50), standard deviation (σ, sorting), skewness (SKI, asymmetry coefficient), and kurtosis (KG, appointment coefficient) were calculated according to the graphic method of Folk and Ward [41]. The granulometric fraction percentages, sediment classification, main statistical parameters, and grain shape are shown in Table S1. Samples were also analyzed by an optical stereomicroscope Leica MZ16 (Leica Microsystems Ltd, Heerbrugg, Switzerland) to identify the shape of quartz and silicate granules embedded in the 384–177 μm range and elaborated with the software TriPlot v.1.4 [42]. In particular, in the sand fraction of 250 μm were counted 100 granules of different shapes for each sample, in total 1000 particles were classified as (1) not abraded, but transparent and angular (NA), (2) blunt-edged translucent, with subrounded to rounded edges, more or less hyaline (BT), and (3) rounded opaque, with well-rounded edges and opaque (RO).

2.4. Simplified new protocol for anthropogenic MPs and MFs counting and description

The samples for the analysis of MPs and MFs were instead collected and allowed to dry in an oven at a temperature of 35 °C for 72 h, and then manually quartered into 1.5 g and SGa_S, SGb_S, TG_S and TG_BE samples were quartered also into 3 g. Double counting on 3 g and 1.5 g was carried out to test if the number of microfibers present in the sample was directly proportional to the weight of the sediments. In all the phases described above, the operating conditions were always carried out ensuring that the sample was not contaminated by external sources. The optical microscopy analyses were conducted in a laboratory without windows, with an air-conditioning system equipped with air filters, maintaining a stable temperature of 23 °C, and with operators wearing sterile cotton lab coats.

After sampling, drying, and manual quartering, the 1.5 g and 3 g of sediment were carefully and homogeneously placed inside a glass of a sterile Petri dish with a diameter of 12 cm, making sure that no heaps were formed, to allow the operator to easily detect the presence of microplastics. Subsequently, the sample was observed in optical microscopy, photographs were taken, and all the fibers and plastics were separated manually from the sediment. For each sample, the microplastic count was performed 3 times (on-site counting).

The samples SGa_BE, SGb_BE, and PO_BE were first photographed in their entirety in the petri dish (20x magnification) and the microfibers contained in the sediments were counted both from images and in live observations, each time repeated three times. This type of approach was performed to verify the correspondence between the on-site counting (directly under the microscope) and the remote counting (image counting; Tables 2a 2b). We have decided to report in Tables 2a 2b the standard deviation and the relative error for each mean of every sample.

The morphological characterization is focused on: color, luster, shape, size, surface roughness as suggested by Lusher et al. [8] and bond with the sediment. For each sample, an Excel sheet was created in which the operator could enter the characteristics observed under the microscope of each MPs and MFs, which was then carefully separated from the sediment.

Regarding morphological analyses on MPs, we decided to adhere to some suggestions outlined in Lusher et al. [8] with additional modifications.

The parameters described were the following:

i) Particle size: Based on existent literature [28,43,8,9], the microplastics can be grouped into size categories. MPs show a dimension between 1 μm and 5 mm, and microfibers (MFs), are thin, elongated MPs with a high length-to-width, ratio of 3:1 or 5:1. Regarding MPs we also chose to measure length (max) and width (max), although the morphologies are often irregular; for MFs length and thickness.

ii) Particle shape: Microplastic particles show highly heterogeneous morphologies and have been described using an equally diverse set of terminologies [8,32]. The definition of MPs shape was based on the presence along the perimeter that delineates the MPs surface of angles (C) or rounded edges (R). MPs defined as 'angular' have only C along the perimeter, 'sub-angular' have a predominance of C over R, 'sub-circular' have a predominance of R over C, and 'circular' have only R. No tire wear particles/anthropogenic rubber particles and spherical and oval disk-shaped MPs were found. We recommend including these shapes in the descriptions as well, noting that tire wear/anthropogenic rubber particles should be placed in a separate category. We described the MFs based on their section as rounded with cylindrical section (named round) and flattened with flat section (named flat).

iii) Color: Generally, the MPs and MFs show homogeneous colors and multiple colors; we described the color based on Lusher et al. [8]; we included the most common colors: red, yellow, black, green, blue, colorless, and white. The color recognition was performed through visual evaluation.

iv) Reflective Properties: We described both transparent, translucent, and opaque. Our observations were carried out using certain measures that allowed us to highlight optical properties such as transparency, translucency, and opacity. We placed a shiny black support, and occasionally a white one (to better observe blue or black microparticles), under a completely transparent borosilicate Petri dish (2 mm thick). In this way, we can observe whether the particles are traversed by light or not. Therefore, in addition to observing the type of luster, which indirectly provides us with information on the transparency, translucency, and opacity of the materials, we can also obtain direct information on these properties. It is important to note that these observations are conducted in reflected light. In many cases, MPs and MFs do not exhibit complete transparency, translucency, or opacity. We have chosen to classify MPs and MFs based on the predominance of one of these surface characteristics.

v) Surface Roughness/Degree of alteration: In this study, the observation was placed on the presence of irregularities on the surface of the MPs (central area) and irregular fringing and/or breaks on the edges of the MPs. Therefore, the MPs were divided into regular, partially irregular, and irregular.

Based on Ocampo et al. [32], the degree of alteration was calculated by considering the portions of the perimeter composed of plain edges (not affected by the presence of angles and roundings; E_{Pl}), rounded edges (E_R), and angular edges (E_C). A predominance of plain edges

Table 2a
Table of results of counting and morphological analyses on MPs in sediments.

	Number	C. %	W. %	O. %	T. %	L. μm	Th. μm	A. %	S.A. %	S.R. %	Round %	R. %	P.I.%	I.%	A.S. %
SGa-S (shoreline)															
Mean 3 g/2	11	27	62	63	37	1064	754	48	29	23	1	31	36	33	14
σ	1	2	2	2	2	145	152	2	1	1	1	1	2	3	2
E.R.%	9	7	2	3	5	13	18	3	3	2	75	3	6	9	11
Mean 1.5 g	10	30	61	64	36	1075	727	46	28	26	1	30	37	33	12
σ	1	1	1	2	2	206	156	1	1	1	1	1	1	0	2
E.R.%	5	3	2	3	6	17	19	1	4	2	75	3	3	0	17
$Mean_{tot}$	10	29	62	64	37	1069	740	47	28	24	1	31	37	33	13
σ	1	2	1	2	2	159	138	2	1	2	1	1	2	2	2
E.R.%	15	10	2	4	7	17	20	4	5	8	75	5	5	9	19
SGa-BE (berm)															
Mean/OM	37	22	50	58	42	766	755	34	41	21	4	28	39	33	13
σ	1	2	2	2	2	325	382	2	2	2	1	2	2	2	1
E.R.%	3	9	3	3	4	41	45	4	5	9	14	5	4	6	8
Mean/live	40	21	51	60	40	887	683	37	41	18	4	28	39	33	13
σ	1	1	1	2	2	295	251	0	2	2	1	2	1	3	1
E.R.%	3	5	2	3	5	31	36	0	5	8	14	7	3	8	4
$Mean_{tot}$	39	22	51	59	41	826	719	36	41	20	4	28	39	33	13
σ	2	2	1	2	2	285	291	2	2	3	1	2	1	2	1
E.R.%	6	9	3	4	6	42	48	7	5	15	14	7	4	8	8
SGb-S (shoreline)															
Mean 3 g/2	11	31	65	54	46	1050	887	49	35	14	1	33	39	28	13
σ	1	1	1	2	2	103	215	1	1	1	1	2	1	3	4
E.R.%	9	2	1	4	4	9	22	2	3	7	100	6	3	11	20
Mean 1.5 g	11	34	61	53	47	961	848	45	37	17	1	33	41	26	14
σ	1	1	1	2	2	186	156	2	1	1	1	1	1	1	2
E.R.%	5	1	2	3	3	17	16	3	3	6	75	3	2	2	11
$Mean_{tot}$	11	33	63	54	46	1006	868	47	36	16	1	33	40	27	13
σ	1	2	2	2	2	143	170	3	1	2	1	1	1	2	2
E.R.%	9	8	4	4	4	16	23	6	4	16	120	6	5	11	19
SGb-BE (berm)															
Mean/OM	40	23	53	58	42	747	321	33	42	23	2	29	38	33	13
σ	2	2	3	2	2	84	97	3	1	5	2	3	1	2	1
E.R.%	5	6	6	3	4	11	30	8	2	19	100	9	3	5	4
Mean/live	41	26	53	58	42	737	627	36	39	24	1	32	40	29	13
σ	1	1	1	3	3	151	91	3	2	1	2	2	0	1	1
E.R.%	2	4	2	4	6	18	13	7	5	4	113	5	1	3	4
$Mean_{tot}$	40	25	53	58	42	742	474	34	40	24	2	30	39	31	13
σ	2	2	2	2	2	109	188	3	2	3	2	2	1	3	1
E.R.%	5	10	6	4	6	18	48	12	7	19	120	12	4	11	4
PO-S (shoreline)															
Mean	3	35	61	54	46	918	785	45	32	22	1	34	40	27	14
σ	1	3	2	2	2	165	65	2	2	3	0	1	3	3	2
E.R.%	33	8	2	4	4	17	7	3	5	14	0	4	7	10	15
PO-BE (berm)															
Mean/OM	12	34	63	64	36	652	531	35	46	19	1	27	39	34	16
σ	2	1	1	2	2	106	158	1	1	1	1	2	2	1	1
E.R.%	13	1	1	2	4	15	28	3	2	3	75	6	5	3	3
Mean/live	15	38	58	64	36	905	657	39	43	17	1	31	36	33	13
σ	1	1	1	3	3	144	211	2	2	1	1	1	1	2	3
E.R.%	3	1	1	4	7	15	29	4	3	3	75	3	3	6	23
$Mean_{tot}$	13	36	61	64	36	778	594	37	45	18	1	29	38	34	14
σ	2	2	2	2	2	179	180	3	2	1	1	3	3	2	2
E.R.%	10	7	4	4	7	32	37	8	6	6	75	12	8	6	21
ER-S (shoreline)															
Mean	5	28	51	63	37	1000	622	31	42	23	4	35	42	23	15
σ	1	3	1	3	3	293	278	1	1	1	1	1	2	1	4
E.R.%	10	7	1	3	5	21	32	3	2	4	25	3	4	2	17
ER-BE (berm)															
Mean	9	36	62	66	35	866	623	33	44	23	1	27	41	32	12
σ	1	1	1	1	1	50	139	0	2	4	1	1	2	1	2
E.R.%	11	1	1	1	1	4	16	0	3	11	100	3	4	3	13
TG-S (shoreline)															
Mean 3 g/2	3	42	31	40	60	973	690	57	26	17	-	51	30	19	21
σ	1	3	2	2	2	24	113	2	4	4	-	2	1	1	1
E.R.%	23	6	5	5	3	2	14	3	14	23	-	4	3	5	3
Mean 1.5 g	3	43	31	43	57	1061	739	62	22	16	-	51	29	20	22
σ	1	4	2	3	3	44	177	3	3	2	-	4	4	1	3
E.R.%	19	8	5	6	4	4	24	4	12	9	-	8	12	5	5
$Mean_{tot}$	3	43	31	41	59	1017	715	60	24	17	-	51	29	20	22
σ	1	3	2	3	3	58	135	3	4	3	-	3	3	1	1
E.R.%	13	8	7	8	6	7	24	8	19	24	-	8	12	8	7
TG-BE (berm)															
Mean 3 g/2	4	44	31	29	71	893	683	31	22	47	-	32	31	37	21

(*continued on next page*)

Table 2a (*continued*)

	Number	C. %	W. %	O. %	T. %	L. μm	Th. μm	A. %	S.A. %	S.R. %	Round %	R. %	P.I.%	I.%	A.S. %
σ	1	4	2	4	4	115	202	1	2	1	-	3	1	2	1
E.R.%	12	9	5	14	6	13	28	3	7	2	-	8	3	5	5
Mean 1.5 g	3	46	32	28	72	752	783	31	22	46	-	29	33	37	23
σ	1	2	1	3	3	91	194	4	2	3	-	3	1	3	1
E.R.%	15	3	3	9	3	12	24	11	7	5	-	9	2	7	4
$Mean_{tot}$	3	45	32	28	72	823	733	31	22	47	-	31	32	37	22
σ	1	3	1	3	3	121	186	2	1	2	-	3	1	2	1
E.R.%	14	9	5	15	6	20	32	11	7	5	-	13	6	7	9

Legend: OM.=microphotographs, C.=colourless, W.= withe, O.=opaque, T. =traslucent, L=length, Th= thickness, A.= angular, S.A.= sub angular, S.R.=sub round, R.=regular, P.I= partially irregular, I.=Irregular, A.S.= association with sediments.

indicates a low degree of alteration (PE_{PL}=1); a predominance of rounded edges indicates a high degree of alteration (PE_R=3); a predominance of angular edges indicates a medium degree of alteration (PEc=2). Additionally, we considered the presence or absence of anomalies in the degree of lustre (A_L) and color (A_C) on the surface of the MPs. A_L and A_C respectively range between 1 (with anomalies) and 0 (without anomalies). The degree of alteration is determined by the combination of perimeter characteristics prevalence and MPs surface conditions (AL and AC). An MP is classified as 'Regular' when the sum of these three values is 1, 'partially irregular' when it is 3, and 'irregular' when it is equal to or greater than 4.

For MFs we consider unaltered microfiber when both the surface and the two terminations will appear regular; partially altered microfiber, when either the surface or one of the two apices will show alterations; in the altered microfiber, we would observe maximum irregularities in both the surface and terminations.

vi) Sediment grains/Relationship with the sediment: This is a new parameter that we have introduced to highlight how methods of separating MPs and MFs, based on gravimetric separation, can sometimes be unreliable. Sediment grains can form a composite particle or become "rafted" along with MPs and MFs. This parameter considers the relationship of the MPs and MFs with the sediment if it was covered and/or trapped between the clasts and could be linked to sediment grain size.

The optical microscope used for counting and morphological characterization of MPs and MFs is the AXIO ZOOM V16 by Zeiss powered by the Museum Center of Natural and Physical Sciences. The objective used is PlanNeoFluar Z 1.0x / 0.25, FWD 56 mm, and the smallest visible structure in the sample is 0.7 μm. The objective can give a magnification ranging from 7x up to 112x. The lighting takes place from a CL 9000 LED CAN with optical annular fiber. The lighting techniques are in reflected light. The AxioCam ICc5 camera was used for image acquisition. The software used is Axiovision SE64 Ref 4.9.1 with Z-Stack, Extended Focus, and Panorama modules. The panorama module was used for comparing the counting and description of MPs and MFs, remotely. 1.5 g of sample in the Petri dish was photographed at 20x magnification, reconstructing the entire area occupied by sediments, MPs, and MFs. Then we treated the dish as if it were a filter.

2.4.1. Data analyses

Statistical analyses were performed using Excel, and IBM SPSS Statistics for Windows (IBM, Version 27.0). Principal Component Analyses (PCA) were performed to explore the association between MFs and MPs numerosity and their characteristics in the different collection sites. The hypothesis on "weight of the samples" and "methods for counting" were compared by using non-parametric Kruskal-Wallis one-way ANOVA on ranks, followed, in case of rejection of the null hypothesis, by Dunn's test ($p < 0.05$). The differences among all sites were performed by one-way ANOVA followed, in case of rejection of the null hypothesis, by Tukey's post-hoc test ($p < 0.05$). The normality and homogeneity of the variances were assessed by Shapiro-Wilk's test and Levene's test, respectively. The Spearman's Rank-Order Correlation test was used to evaluate the correlation between the MFs and MPs number and their characteristics.

2.5. Detailed morphological and qualitative chemical analysis (SEM-EDS[1])

SEM-EDS analyses were carried out on SGa_S, SGa_BE, SGb_S, SGb_BE, PO_S, PO_BE, ER_S, and ER_BE samples, to obtain information about the chemical nature of the MFs in sediments [44,35,45-50] (Fatemina et al., 2023), to detect the presence of pollutants on the surface of the microfiber and to confirm the morphological data collected in OM (*shape*, *Surface Roughness and Sediment Grains)*. Detailed morphological and semi-quantitative chemical analyses of microplastic samples were performed by using a scanning electron microscope (SEM) JEOL-JSM 5310 at CISAG, University of Naples Federico II, coupled with energy dispersive X-Ray spectroscopy (EDS). The setup is equipped with an Oxford Instruments Microanalysis unit: INCA X-act detector and operating at 15 kV primary beam voltage, 50–100 mA filament current, variable spot size, 20 mm WD, and 40 s net acquisition real-time. INCA X-act detector uses Energy software with an XPP matrix correction scheme and Pulse Pile-up correction. The data were processed with INCA software version 4.08 [51]. For semi-quantitative chemical analyses, the samples have not been coated. 10 analytical points for each sample were collected; morphological analyses were performed, after coating the sample with gold.

2.6. Raman microspectroscopy

The chemical nature of the MFs in sediments can be efficiently investigated by Raman spectroscopy [52,53]. Herein, RAMAN microspectroscopy analyses were performed on MFs from 6 sampling sites (SGa_S, SGa_BE, SGb_BE, PO_S, PO_BE, ER_BE). The individual MFs, manually separated, were fixed on a sterile slide using a thin layer of gum arabic. In some cases, to reduce fluorescence an aluminum foil was placed underneath the sample [54]. One of the fiber tips was embedded, leaving the rest of the surface free from any interference. The sample was not treated with any substance to avoid alterations. A confocal Raman microscope (Jasco, NRS-3100) was used to obtain Raman spectra. The 514 nm line of an air-cooled Ar^+ laser (Melles Griot, Rochester, NY, USA, 35 LAP431 220) was injected into an integrated Olympus microscope and focused on isolated fibers with a laser spot diameter of approximately 1–5 μm. A 20X–100X objective with a final 2 mW power at the sample was used. A holographic edge filter was used to reject the excitation laser line. Raman backscattering was collected using a diffraction lattice of 1200 grooves/mm and 0.1 mm × 6 mm slit, corresponding to an average spectral resolution of up to 7 cm^{-1}. Because of the fluorescence of the samples, the acquisition time was not the same for all. In some cases, a time of about 10–60 s was required to collect a complete dataset from a Peltier-cooled 1024 × 128-pixel CCD photon detector (Andor DU401BVI). Raman measurements were carried out in triplicate for reproducibility for each spot sampled. Wavelength calibration was performed by using cyclohexane as a standard. Raman

[1] "SEM" stands for " Scanning Electron Microscopy" and "EDS" stands for " energy dispersive X-Ray spectroscopy."

Table 2b
Table of results of counting and morphological analyses on MFs in sediments.

Number	C. %	W. %	O. %	T. %	L. μm	Th. μm	Flat%	Round %	R. %	P.I.%	I.%	A.S. %
SG1-S (shoreline)												
Mean 3 g/2	194	50	36	42	58	1513	17	83	17	46	36	19	63
σ		3	4	5	5	325	2	4	4	2	3	1	2
E.R.%	4	7	10	11	8	19	12	4	21	4	8	5	3
Mean 1.5 g	182	47	33	42	58	1625	19	85	15	43	35	22	62
σ	6	3	2	6	6	357	2	5	5	3	5	2	2
E.R.%	3	6	5	14	10	20	11	6	33	7	13	9	3
$Mean_{tot}$	188	48	35	42	58	1569	18	84	16	44	36	21	63
σ	9	3	3	5	5	311	2	4	4	3	3	3	2
E.R.%	7	9	10	14	10	23	17	6	32	9	13	15	4
SG1-B (berm)												
Mean/OM	451	55	34	42	58	466	16	43	57	38	36	26	22
σ	19	5	3	3	3	74	1	3	3	2	3	2	2
E.R.%	4	8	9	7	5	15	6	6	5	4	8	6	9
Mean/live	482	52	33	45	55	487	17	46	54	38	34	28	12
σ	21	2	2	4	4	68	2	3	3	2	4	4	2
E.R.%	4	4	6	9	7	14	9	6	5	5	10	14	16
$Mean_{tot}$	466	54	33	43	57	476	16	45	55	38	35	27	17
σ	25	4	2	4	4	64	1	3	3	2	3	3	6
E.R.%	8	8	9	12	9	15	9	9	7	5	13	15	41
SG2-S (shoreline)												
Mean 3 g/2	179	47	39	44	56	1251	17	77	23	41	47	12	38
σ	6	4	5	2	2	207	2	3	3	3	2	1	3
E.R.%	3	7	12	5	4	15	12	3	11	7	4	10	7
Mean 1.5 g	170	49	39	45	55	1211	22	86	14	39	51	10	39
σ	5	3	2	3	3	308	2	3	3	1	1	1	4
E.R.%	3	5	5	6	5	23	9	4	21	3	2	5	9
$Mean_{tot}$	175	48	39	44	56	1231	20	81	19	40	49	11	38
σ	7	3	3	2	2	236	3	5	5	2	3	1	3
E.R.%	5	8	12	6	4	23	23	9	38	7	7	13	9
SG2-B (berm)												
Mean/OM	527	52	41	46	54	747	13	38	62	34	40	26	29
σ	24	3	4	4	4	84	2	3	3	2	4	2	6
E.R.%	4	5	10	8	6	11	15	8	5	6	9	8	20
Mean/live	534	55	36	47	53	741	13	37	63	36	42	22	28
σ	14	3	2	2	2	174	1	4	4	1	3	3	3
E.R.%	3	5	5	4	4	23	4	11	7	1	7	11	9
$Mean_{tot}$	531	53	39	46	54	744	13	38	62	35	41	24	29
σ	18	3	4	3	3	122	2	3	3	2	3	3	4
E.R.%	5	8	15	8	7	23	15	11	7	7	10	17	21
PO-S (shoreline)												
Mean	83	70	22	34	66	1218	18	82	18	34	46	20	54
σ	4	2	3	2	2	196	8	2	2	1	4	3	8
E.R.%	5	2	11	6	3	16	41	2	10	4	8	14	15
PO-B (berm)												
Mean/OM	166	74	21	24	76	485	15	85	15	31	42	27	58
σ	6	2	2	3	3	46	1	3	3	2	2	3	2
E.R.%	4	2	7	11	3	9	7	4	20	5	5	9	3
Mean/live	172	68	24	25	75	652	13	84	16	34	43	22	61
σ	4	3	4	3	3	121	2	3	3	2	2	4	5
E.R.%	2	4	16	12	4	18	16	3	18	6	5	16	7
$Mean_{tot}$	169	71	23	24	76	568	14	85	15	32	43	25	59
σ	6	4	3	3	3	123	2	3	3	2	2	4	4
E.R.%	4	7	20	14	5	30	18	4	23	9	6	20	8
ER_S (shoreline)												
Mean	97	68	27	33	67	1148	21	89	11	35	52	13	55
σ	7	4	4	4	4	139	2	3	3	3	4	2	5
E.R.%	7	5	15	11	5	12	7	3	22	7	8	11	9
ER_BE (berm)												
Mean	120	65	27	37	64	866	18	79	21	29	47	24	57
σ	5	1	1	3	3	31	3	4	4	3	3	6	5
E.R.%	4	2	4	7	4	3	16	5	19	9	6	22	6
TG_S (shoreline)												
Mean 3 g/2	85	50	30	27	73	1973	18	41	59	45	37	18	25
σ	1	4	1	2	2	361	2	2	2	2	6	4	4
E.R.%	1	8	3	8	3	18	11	4	3	4	16	22	14
Mean 1.5 g	76	50	27	27	73	2061	19	45	55	45	37	18	26
σ	2	4	3	4	4	234	4	4	4	1	4	4	4
E.R.%	3	7	11	14	5	11	21	8	6	2	9	19	13
$Mean_{tot}$	81	50	28	27	73	2017	19	43	57	45	37	18	26
σ	5	4	3	3	3	277	3	3	3	2	4	3	4
E.R.%	8	9	12	14	5	18	21	10	7	5	16	22	14
TG_BE (berm)												
Mean 3 g/2	75	48	29	25	75	1529	15	30	70	43	27	30	22

(*continued on next page*)

Table 2b (*continued*)

Number	C. %	W. %	O. %	T. %	L. μm	Th. μm	Flat%	Round %	R. %	P.I.%	I.%	A.S. %
σ	4	2	2	2	2	233	4	3	3	1	1	1	2
E.R.%	5	3	5	8	3	15	24	8	4	1	4	2	7
Mean 1.5 g	67	47	30	28	72	1657	16	29	71	43	27	29	23
σ	2	1	2	2	2	101	3	3	3	2	2	1	4
E.R.%	3	2	7	7	3	6	19	10	4	3	8	2	15
$Mean_{tot}$	71	47	30	26	74	1593	15	29	70	43	27	30	23
σ	5	1	2	3	3	175	3	2	3	1	2	1	3
E.R.%	10	3	7	14	5	15	23	10	4	3	8	3	16

Legend: OM.=microphotographs, C.=colourless, W.= withe, O.=opaque, T. =traslucent, L=length, Th= thickness, R.=regular, P.I= partially irregular, I.=Irregular, A.S.= association with sediments.

spectra were registered in the range of 100–2100 cm^{-1} for 30 randomly selected MFs samples. Inspection via optical microscopy allowed us to identify micrometric areas for Raman investigation. Raman assignment was based on the acquisition of microplastic reference Raman spectra (Fig. S1) collected from the Polymer Kit 1.0 of Hawai'i Pacific University (Center for Marine Debris Research), together with specific literature on microplastic and microfibers [55-58].

3. Results and discussion

The presentation of the results was conducted following the scheme outlined in Fig. 2.

3.1. Sedimentological analysis

Sediment classification (Table S1) shows mainly medium sand followed by coarse sand (SGa_BE, SGb_BE), a texture very poor in gravel and a very fine fraction (<63 mm) dominated by sand and secondly slightly gravelly sand (SGa_S, PO_BE, TG_BE). The grain mean size (Mz) ranges from 1.98 and 0.33 f of medium sand and coarse sand (SGa_BE, SGb_S), generally unimodal or bimodal (SGb_S, SGb_BE). The sorting (s) varies from moderately sorted (SGa_S, SGb_BE) to moderately well sorted (TG_S, TG_BE, PO_S, PO_BE) and well sorted (ER-S, ER-BE). The skewness (S_{KI}) is mainly symmetrical followed by coarse (SGa_S, PO_S), fine (SGa_BE), and very fine skewed (SGb_BE) deposits. Finally, the kurtosis (K_G) of these beach sands is mainly mesokurtic and secondarily platykurtic (SGb_S, SGb_BE). The results are summarized in the granulometric spindle of cumulative frequency curves of the beach from northwest to southeast (Fig. S2a).

The grain size fraction of the sand depends on the hydrodynamic environment and influences the transport of MPs and MFs, while mineralogical composition does not. Along the shoreline, where the sand grains are coarser, and there is constant transport and washout by sea waves, the number of MPs and MFs is generally lower than that recorded in the berm. Instead, in the berm, the accumulation is due to the few waves that have shaped it but above all to the wind that blows from the sea towards the upper part of the emerging beach. Thus, wave and wind dynamics, influencing the sand fraction, are key in determining the distribution of MPs and MFs on beaches. For this reason, we sampled sediments in these two main beach zones.

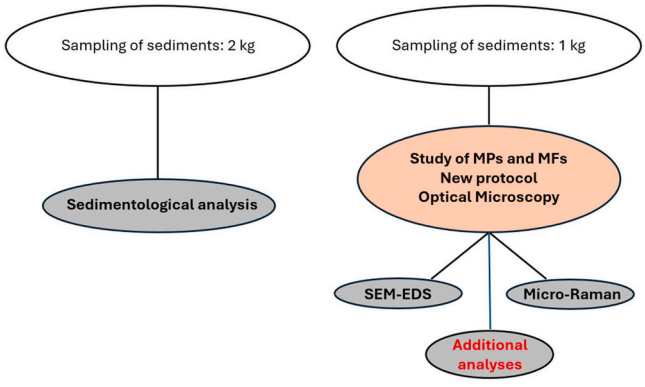

Fig. 2. Protocol outline: The protocol involves a double sediment sampling, one for sedimentological analyses and one for MPs and MFs analyses. Subsequently, analyses are carried out simultaneously. After characterizing MPs and MFs on manually separated microparticles, further analyses can be conducted; in our case, we performed analyses using EDS-SEM and Micro Raman techniques.

In the sand fraction of 250 mm were also observed bioclasts of mollusks, ostracods and foraminifers, echinoid spines, clay material, and MPs and MFs.

Distribution of the three different morphoscopic classes of quarts and silicate grains shows: not abraded grains count the highest value of 582 elements (NA 58 %); blunt-edged type follows with 303 granules (BT 40 %); finally, rounded opaque are the less common with only 20 grains (RO 2 %) The results are shown in the triangular diagram (Fig. S2b) with grouping of the two main sets and the outlier ER_BE. Different from others, the last sample contains the lowest number of 21 NA grains, the highest one of 73 BT granules, and a significant number of 6 RO elements (Table S1).

The sand fraction of 250 mm is seasonally transported by sea waves, marine currents, wind, and rivers on the beach from the water system [10,59,60,28,61-64]. Distribution of the three different morphoscopic classes of quartz and silicate grains recognized in the sediments allows us to identify their genetic-depositional environment. In particular, not abraded grains indicate a short transport with poor erosion typical of a beach at the cliff foot; blunt-edged type is representative of the river mouth, emerged-submerged beach environment; finally, rounded opaque grains, the less common, are attributable to a coastal dune or due to many cycles of inshore-offshore motion by sea waves along the beach. Considering that currently there is no coastal dune in the studied area, these few grains witness a palaeo dune environment, as that found in the underground of the southeastern sector of Naples 5 km to the northwest, or likely were rounded by repeated wave and wind modeling through corrosion along the foreshore. The ERL2 sample, differently from others, shows that beach exposition to wave cycles approaching the littoral in a NW-oriented short geographic fetch (over 700 km).

3.2. MFs and MPs counting applying the simplified new protocol on sediments

The method here proposed does not involve initial sieving processes; therefore, the collected material is analyzed as it is, without losing any particle size fraction [28].

The count performed on 3 g of sediment compared to the count performed on 1.5 g, for SGa_S, SGb_S, TG_S, and TG_BE samples, indicates consistent data with no differences between the two counts (i.e., the 3 g counts halved gave statistically similar results as for 1.5 g counts; Fig. 3A, B).

The count performed on the data collected from images (OM) compared to the count live (live) performed indicates no statistical differences between the data provided by the two approaches (Fig. 3C, D).

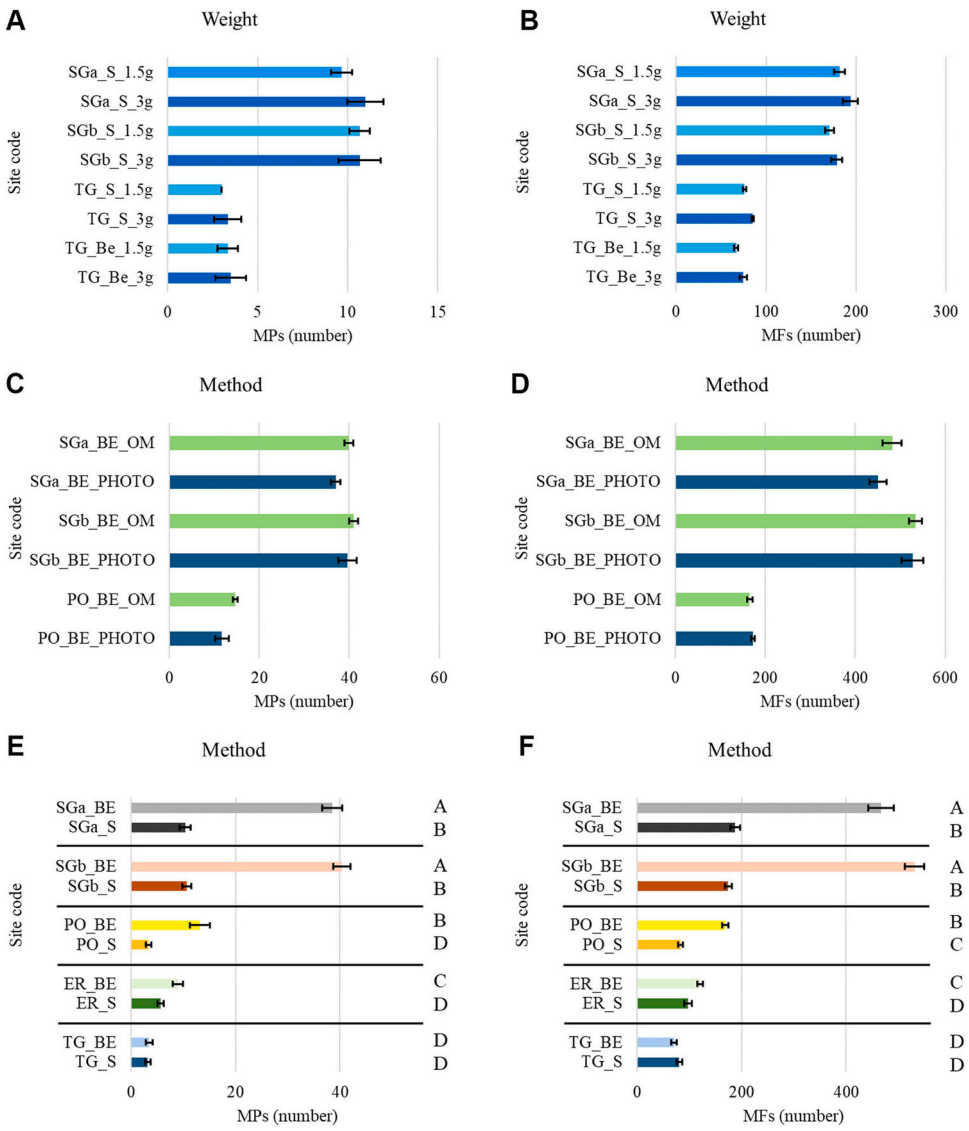

Fig. 3. Bar charts of MPs and MFs number to compare the effect of weight of the sample, 1.5 or 3 g (**A** and **B**), the observation method (**C** and **D**) and all sites together (**E** and **F**). Bars are the average values, and the error bars the standard deviations. Different letters indicate significant differences according to Tukey's test, $p < 0.05$. As for weight of the sample and observation method, the pairwise comparison gave no statistical difference (e.g., sample of 3 g (halved) Vs. 1.5 g and sample Photo Vs. OM, see M&M for details).

Except for the TG sites, the sampling points near the berm were the most affected by MPs and MFs contamination. Furthermore, from the statistical comparison, it emerged that the SG sites are on average more impacted than the other sites, followed by PO> ER> TG, and this is for both MFs and MPs (Fig. 3E, F).

The calculated errors and statistical analyses confirm the validity of the analytical methodology under experimentation. However, we have still reported in Tables 2a the collected descriptions with standard deviations and relative error for MPs, which show a good correlation between the values. The total count (six times) of MFs for each sediment sample for each methodology (three times) shows a standard deviation and relative error, in a good correlation. Tables 2b presents the means, standard deviations, and relative errors for all types of measurements (live, imaging, and 1.5 g, 3 g), sample by sample, for all the parameters described. Quantitative analyses on parameters such as color, luminosity, dimensions, shape, degree of alteration, and association with sediments based on the different amounts (1.5 or 3 g) of sediment analyzed and the type of acquisition (live and on microphotographs) are comparable, as evidenced by Tables 2a 2b.

The number of microplastics was very low ranging from 3 (PO_S, TG_S, and TG_BE) to 40 (SGb_BE). Microfibers represent a total of 96 %, while the remaining 4 % is represented by fragments of microplastics following Harris [28].

The sizes of the fragments on the berm are on average 807 μm in length and 631 μm in width (1.28 mm^2). While those on the foreshore show on average a length of 1006 μm and a width of 741 μm (1.92 mm^2). Regarding the shape of MPs (Fig. 4) on the berm, they are sub-angular in 38 % of cases, angular in 34 %, sub-rounded in 26 %, and rounded in 1 %; on the foreshore, in 49 % of cases, they are angular, in 30 % sub-angular, in 21 % sub-rounded, and 1 % rounded.

The most prevalent color is white (54 %), along with colorless (34 %), while colored MPs are present at a rate of 12 %. 55 % of MPs are opaque, while the remaining 45 % are translucent (Fig. 4A and C). There are no differences between the berm and the foreshore for optical properties. As for the degree of alteration, MPs on the berm appear to be slightly more altered (regular 29 %) than those on the foreshore (regular 36 %). Finally, regarding the parameter related to interaction with sediment clasts, the value is ~ 14 % (Fig. 4C).

Comparing the morphological description of MPs with the classification and categorization of MPs and MFs reported in Yu et al. [30], we

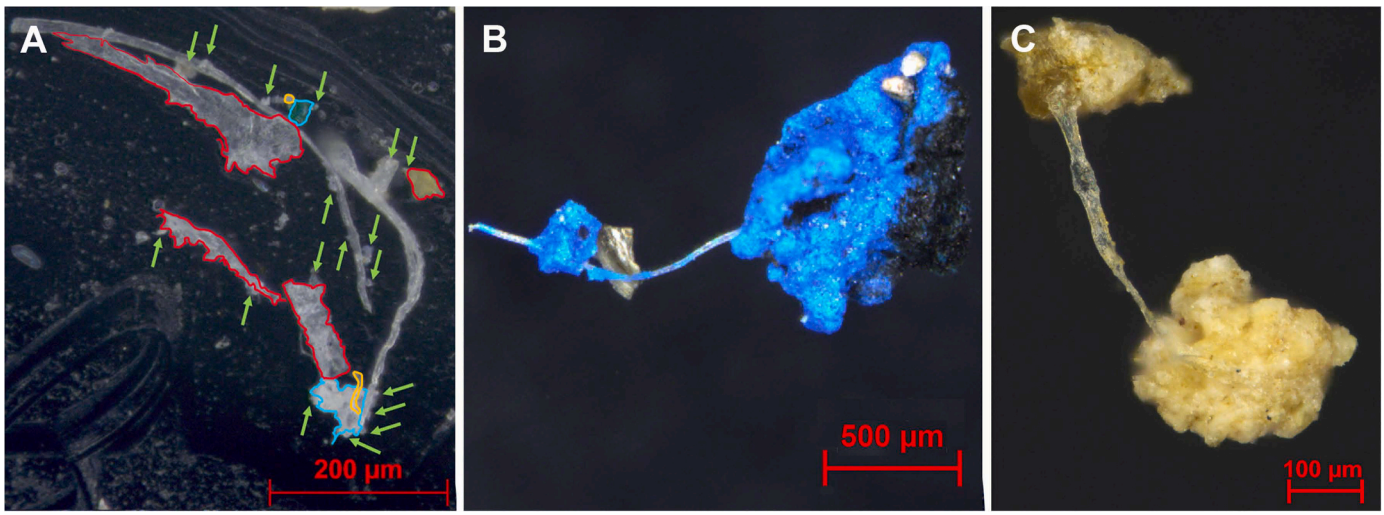

Fig. 4. Images in stereomicroscopy of MPs fragments. **A.** The larger fragments exhibit angular to sub-angular morphologies, are colorless and translucent. White and yellow fragments can also be observed. The largest fragment appears partially altered. The green arrows indicate the presence of inorganic clasts on the edges of the MPs and MFs. In red, yellow, and cyan, we highlighted the perimeter of the MPs. **B.** Sub-angular fragments of blue and black MPs associated with a MF. It is possible to observe some sediment micro clasts on the surface (top right). **C.** Fragment of microplastic firmly anchored to the sediment. The MP is colorless, translucent, and unaltered.

hypothesize that the samples contain:

- "fragments," characterized by angular shapes, angular edges, often scraped, abraded, broken, and sheared in random directions, opaque or translucent;.
- "films," characterized by sub-angular shapes, angular and rounded edges, translucent or transparent but occasionally opaque;.
- "irregularly shaped microbeads", characterized by sub-rounded shapes with rounded edges, sometimes with angular edges, white or clear in color, opaque or translucent;.
- rarely, "spherical microbeads", characterized by rounded shapes, opaque or translucent.

The higher abundance of microfibers compared to microplastics has prompted us to develop a characterization protocol for MFs that is slightly different from the one previously outlined for MPs, with modifications mainly related to the morphology of the samples, which is absent in existing studies, as described in the Materials and Methods section.

Regarding the characterization performed through optical microscopy on the MFs present in the sediments, we can say that: for the parameter related to optical features, the prevalent colors are colorless (57 %) and white (30 %), for luster the prevalent trait is translucent (64 %) (Fig. 5A, B, C, E, F and G) over opaque (36 %) (Fig. 5D, and 5H). The length of the microfibers on the berm averages 850 µm, with a thickness of 15 µm, while on the shoreline, they average 1437 µm in length and 19 µm in thickness. For shape, we recognize flat (Fig. 5A, C, D, E, F) and round (Fig. 5B, G and H) MFs; The percentage of flat MFs on the berm is 55 % and on the shore is 76 %, while the percentage of round ones is 45 % on the berm and 24 % on the shoreline. In many cases, flat MFs coil and fold back onto themselves. Comparing the morphological description of MFs with the classification and categorization of MPs and MFs presented in Yu et al. [30], we can hypothesize that the samples contain both polyester fibers, characterized by a rounded shape, light color and consistent thickness and shape, and organic fibers, such as silk, described as flat MFs twisted with constant width.

The longer MFs are more associated with the shoreline (Fig. 6A). This is most likely due to the pollution source originating from the sea. Therefore, on the shoreline, we can consider the MFs recently produced, while on the berm, the MFs undergo greater alteration, both chemically (exposure to sunlight and rain) and mechanically (transport, wind, dragging due to adverse weather conditions), therefore, they appear smaller. Furthermore, in this stretch of the shoreline, there is greater hydrodynamic energy due to wave motion and the breezes from the land, which continuously mix the sediments. The greatest occurrence of small MFs on the berm is likely due to the action of wind which carries them more easily inland, but also to exceptional storm surges. This is congruent with the observed degree of alteration, which is generally lower for MPs and MFs found on the shoreline (Fig. 6).

AS for MFs alteration (Fig. 5C, D, E), they are on average 29 % regular on the berm and 36 % on the shoreline, 38 % are partially irregular (both in the berm and shoreline), and those irregulars are 33 % on the berm and 26 % shoreline. Without any digestion process, often conducted with hydrogen peroxide, smaller particles, but especially MFs, are unlikely to undergo surface alteration or dissolution processes (Hurley, 2018). Therefore, we can obtain accurate and detailed information on the actual degree of alteration, length, thickness, color, etc., simply using microscopy techniques (OM, SEM, TEM), and on the presence of any bacterial colonies and/or organic materials, films of heavy metal pollutants, mineralogical composition of sediments present on the coast, using various analytical methodologies (SEM-EDS, FT-IR, Raman, bacterial cultures, etc.).

MFs were differently associated with the sediments, on average for 37 % to the berm sediment and 47 % to the shoreline sediment (Fig. 5F, 5G, 5H). This method, considering the parameter 'Association with sediments', highlights how gravity separation could incur non-trivial issues, causing the loss of material in the final count of MPs, especially of MFs (Lusher, 2020). The loss from the collected data could be around ~15 % for MPs and ~40 % for MFs, this is especially true for flat MFs.

Furthermore, this methodology has allowed us to highlight some correlations among the studied parameters, consistently attributable to the depositional dynamics of MFs.

Interesting correlation and association observed stem from the shape of the MFs and their connection with sediment, supported by Spearman correlation matrices and PCA (Fig. 6A and Table 3 a1 and a2). The flat microfibers exhibit a strong bond with the sediments both on the berm and on the shoreline, unlike the round microfibers. The larger surface area of flat MFs renders them more susceptible to these forces, potentially facilitating their burial or embedding within sediment layers over time. In contrast, round MFs, with their smooth and slender morphology, are less resistant to hydrodynamic forces, leading to increased suspension in the water column. Furthermore, the different morphology of the microfibers could lead to various types of biological interactions. Flat microfibers, with their structure, might be more prone

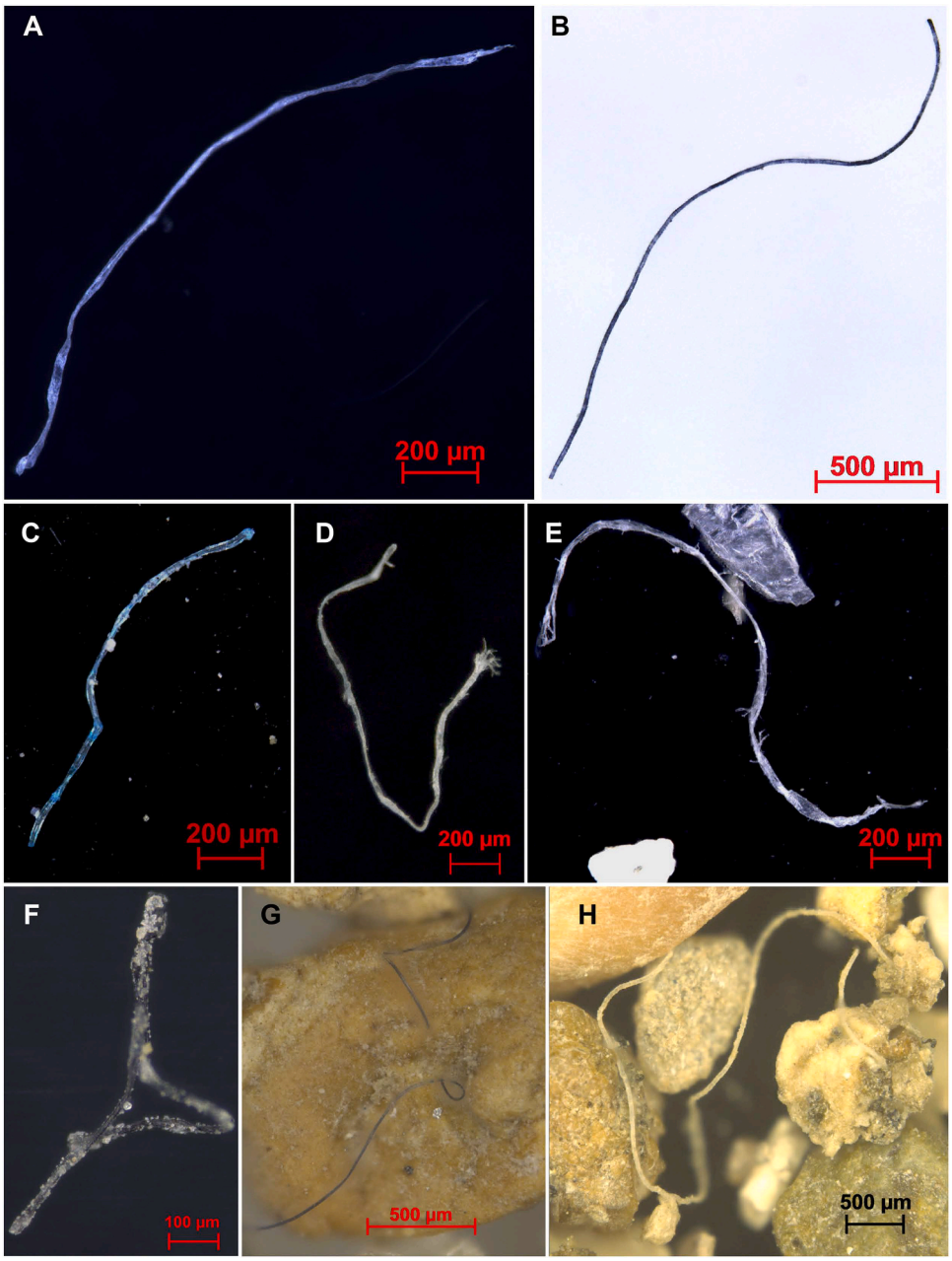

Fig. 5. Images in stereomicroscopy of MFs. **A**. Flat, translucent, and partially altered. **B**. Round, translucent unaltered. **C**. Flat, translucent, blue unaltered MFs covered by micro fragments of sediments. **D**. Flat, opaque, with, partially altered MFS. **E**. Flat, translucent withe, altered. **F**. Flat, colourless, translucent, unaltered covered by sediments micro fragments. **G**. Round, translucent, blue, unaltered firmly anchored to the sediment. **H**. Round, opaque, white, covered by micro fragments of sediments and attached to macro grains.

to interactions with organisms, such as microbial communities. Rounded microfibers, due to their less intricate nature, may be less attractive to certain biological entities, resulting in weaker attachments.

The PCA analyses (Fig. 6) confirm a difference between the characteristics of microplastic particles (MPs) and microfibers (MFs) found on the foreshore (abbreviated as S) and on the berm (abbreviated as BE); for example, MFs found on the BE exhibit a higher degree of alteration and smaller sizes compared to those found on the S. Furthermore, they highlight that the San Giovanni site (SG) has the highest number of MPs and MFs, while the Torre del Greco site (TG) presents anomalies in the morphological characteristics found in the other sites (e.g., morphological characteristics of the BE site very similar to those of the S site). A case of particular importance is given to samples TG-S and TG-BE, for which the count was carried out 6 times each (3 for 1.5 g and 3 for 3 g). In this case, the number of fragments of MPs and MFs is very similar for the shoreline and the berm (Fig. 3E, 3F, 6A, and 6B). Indeed, sampling of the berm was conducted in an area facing the open sea from both sides (NW and SE). This area is therefore more exposed to tides and winds that carry away both MPs and MFs. These data confirm the effectiveness of the method, which provides fundamental information on the dynamics of accumulation of MPs and MFs, which likely follow the dynamics of accumulation of coastal marine sediments.

From the data analysis, another interesting correlation among the described parameters is provided by shape, color, optical properties, and the degree of alteration.

Flat MFs are the most abundant, especially on the shoreline, generally colorless and smaller in size, especially on the berm; they are moderately altered and show a stronger association with sediments.

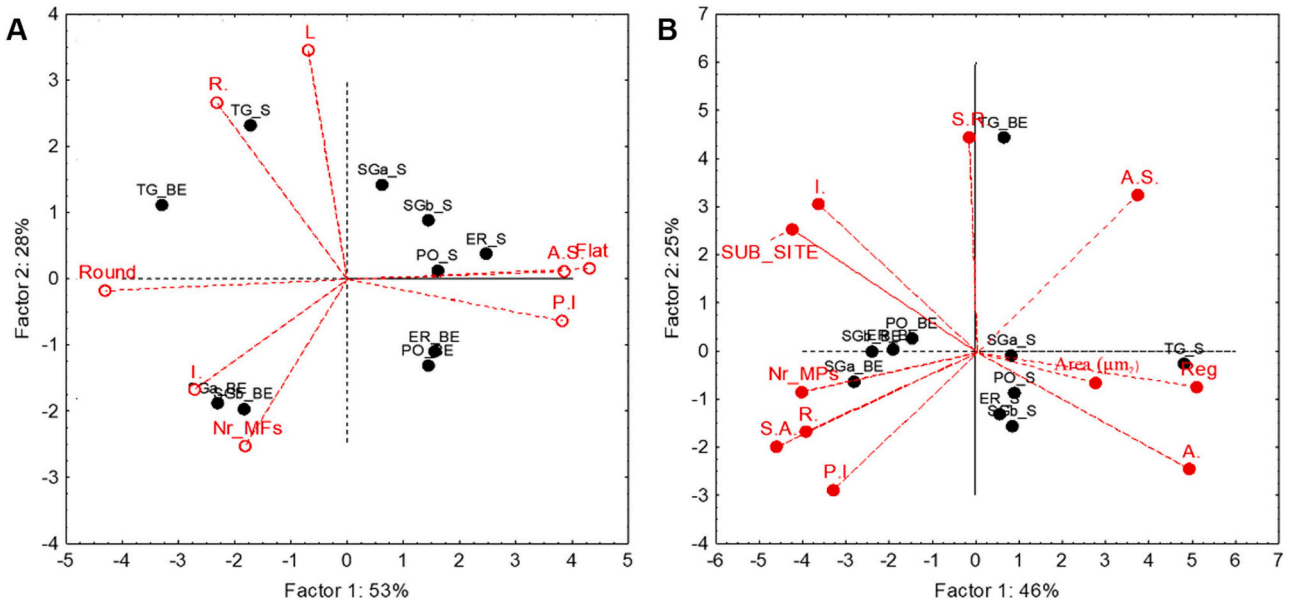

Fig. 6. PCA of MFs (**A**) and MPs (**B**) number and their characteristics. In black collection sites; in red loading vectors of MFs and MPs characteristics. **Legend for MFs**: L=length, R.=regular, P.I= partially irregular, I.=Irregular, A.S.= association with sediments. **Legend for MPs**: A.= angular, S.A.= sub angular, S.R.=sub round, R.=regular, P.I= partially irregular, I.=Irregular, A.S.= association with sediments.

Round microfibers are less common, especially on the shoreline, longer, with a lower degree of alteration, and weakly associated with sediments. Additionally, even though statistically the data is not significant, on the shoreline they are translucent while on the berm they are opaque (Table 3 a1 and a2). Furthermore, spearman correlations show that round microfibers on the shoreline are translucent and less altered, while on the berm they become opaque and more altered; conversely, flat microfibers exhibit the opposite trend for optical features but are always more altered (Fig. 6A). These characteristics are often linked to the chemical nature of the microfibers (MFs) and to their morphology. The more altered MFs may be of natural origin, such as wool, cotton, silk, etc., while those more resistant may be of a polymeric nature (nylon, PPs, PVC, etc.). These data are consistent with the chemical analyses (EDS and MicroRaman) conducted on a representative sample of microfibers (MFs).

The Spearman correlation matrices highlight correlations among morphological characteristics of microplastics (Table 3 b1 and b2); for example, on the shoreline, concerning MPs, they are sub-angular generally white and opaque, and more altered. MPs on the berm, however, are angular generally opaque and less altered (Fig. 6B).

This analytical methodology has allowed us to highlight important depositional dynamics of MFs and MPs for the first time, and, more importantly, it enables us to reconstruct the locations of pollutant sources and assess their impact on the coastlines.

As evident from the data, the accumulation of MPs and MFs follows the normal depositional trends of sediments according to the coastal marine currents. The MPs and MFs are mainly introduced by coastal currents and storm surges. The presence and orientation of coastal breakwaters influence the accumulation of these materials, the specific weight of which is lighter than that of the sediments of these beaches. All three urban beaches are exposed to storm surges from S-W (libeccio) and S-E (sirocco) with an extensive geographic fetch (over 700 km). The MFs and MPs are more present on the storm berm than on the shoreline because the berm is the site of sediment accumulation (Fig. 3E and 3F; Tables 2a 2b).

Data reveal, particularly in San Giovanni a Teduccio beach, a notably higher concentration of MFs and MPs (Fig. 3E and 3F), due to anthropogenic influences and its greater exposure to sea waves. These sediments statistically are attributable to a beach, even if their parameters suggest a sea-wave polycyclic rework as for dune grains remodeled by wind, an environment today absent in this site but once present in the Late Pleistocene, and a poor river supply.

This anomaly is attributed to the proximity of industrial activities and the presence of the port of Naples, which releases pollutants into the surrounding waters, and to a sewage treatment plant which is located 5.9 km away and which has not been adapted to standards yet, the illegal connections to the sewer system and unsuitably treated urban discharges. Ercolano, Portici, and Torre del Greco move away from the most polluted area and do not have streams in their vicinity, so the MFs and MPs only come from the sea and occasionally from runoff (Fig. 1). In Portici, we could find in some conditions a fairly large number of MPs and MFs as it is more exposed to the sea storms from SE, while Ercolano has the least amount because it is sheltered from the storm surges coming from the SW and the SE precisely by the coastal defense works, as the morphology of the beach itself suggests. Interestingly, Capozzi et al. [56], studying the deposition of airborne anthropogenic microfibers in natural and seminatural sites of the Campania region, found a higher number of microplastics and longer fibers near the sites closer to urbanized areas, likely as the results of continuous flux from nearby sources; this finding is in line with the close association between MFs characteristics and abundance found in the present work in sediments collected in sites not distant from the sites of the work by Capozzi et al. [56].

Data on localized pollution hotspots due to anthropogenic inputs underline the need for targeted mitigation strategies in those areas with high industrial presence. As we move away from the source and head south, the concentrations of MPs and MFs decrease, highlighting how longshore currents, mainly NW-SE oriented, push pollutants from the industrial areas of the Port of Naples towards the southern coasts. In fact, in Torre del Greco, located 8 km south of the most polluted beach in San Giovanni a Teduccio, the MFs decreased by about 5 times.

The morphological characteristics highlighted by the microplastics indicate not only accumulation dynamics due to natural phenomena such as marine and aeolian transport and erosion (previously described for MFs) but also input from the mainland, as these are beaches located along heavily anthropized coastlines.

Regarding the analysis timing, we need to emphasize that to count a 1.5-g sample once, an experienced operator may take 1 to 2 h,

Table 3
Spearman R correlation matrices between MFs (a1-S and a2-BE) and MPs (b1-S and b2-BE) number and their characteristics. Significant correlations are marked ($p < 0.05$). Legend: C.=colourless, W.= withe, O.=opaque, T. =traslucent, L=length, R.=regular, P.I= partially irregular, I.=Irregular, A.S.= association with sediments, A.= angular, S.A.= sub angular, S.R.=sub round.

a1)

Shoreline	Nr_MFs	C.	W.	O.	T.	L	Flat	Round	R.	P.I	I.	A.S.
Nr_MFs	1,00	−0,43	0,76	0,75	−0,75	−0,25	0,46	−0,46	0,17	−0,08	−0,08	0,66
C.	−0,43	1,00	−0,74	−0,47	0,47	−0,12	0,34	−0,34	−0,62	0,45	−0,02	0,10
W.	0,76	−0,74	1,00	0,74	−0,74	−0,17	0,08	−0,08	0,31	−0,03	−0,36	0,13
O.	0,75	−0,47	0,74	1,00	−1,00	−0,47	0,34	−0,34	0,01	0,16	−0,24	0,46
Tr.	−0,75	0,47	−0,74	−1,00	1,00	0,47	−0,34	0,34	−0,01	−0,16	0,24	−0,46
L	−0,25	−0,12	−0,17	−0,47	0,47	1,00	−0,44	0,44	0,45	−0,55	0,39	−0,35
Flat	0,46	0,34	0,08	0,34	−0,34	−0,44	1,00	−1,00	−0,56	0,51	−0,23	0,67
Round	−0,46	−0,34	−0,08	−0,34	0,34	0,44	−1,00	1,00	0,56	−0,51	0,23	−0,67
Reg	0,17	−0,62	0,31	0,01	−0,01	0,45	−0,56	0,56	1,00	−0,83	0,34	−0,19
P.I	−0,08	0,45	−0,03	0,16	−0,16	−0,55	0,51	−0,51	−0,83	1,00	−0,77	0,01
I.	−0,08	−0,02	−0,36	−0,24	0,24	0,39	−0,23	0,23	0,34	−0,77	1,00	0,25
A.S.	0,66	0,10	0,13	0,46	−0,46	−0,35	0,67	−0,67	−0,19	0,01	0,25	1,00

a2)

Berm	Nr_MFs	C.	W.	O.	T.	L	Flat	Round	R.	P.I	I.	A.S.
Nr_MFs	1,00	0,15	0,66	0,72	−0,72	−0,50	0,14	−0,14	−0,28	0,33	−0,50	−0,08
C.	0,15	1,00	−0,56	−0,20	0,20	−0,60	0,88	−0,88	−0,77	0,71	−0,44	0,74
W.	0,66	−0,56	1,00	0,77	−0,78	0,06	−0,52	0,52	0,30	−0,20	−0,15	−0,55
O.	0,72	−0,20	0,77	1,00	−1,00	−0,19	−0,25	0,24	−0,01	0,05	−0,20	−0,38
Tr.	−0,72	0,20	−0,78	−1,00	1,00	0,19	0,24	−0,24	0,01	−0,05	0,20	0,38
L	−0,50	−0,60	0,06	−0,19	0,19	1,00	−0,61	0,61	0,34	−0,20	0,22	−0,06
Flat	0,14	0,88	−0,52	−0,25	0,24	−0,61	1,00	−1,00	−0,71	0,68	−0,42	0,59
Round	−0,14	−0,88	0,52	0,24	−0,24	0,61	−1,00	1,00	0,71	−0,68	0,43	−0,59
Reg	−0,28	−0,77	0,30	−0,01	0,01	0,34	−0,71	0,71	1,00	−0,87	0,43	−0,72
P.I	0,33	0,71	−0,20	0,05	−0,05	−0,20	0,68	−0,68	−0,87	1,00	−0,76	0,75
I.	−0,50	−0,44	−0,15	−0,20	0,20	0,22	−0,42	0,43	0,43	−0,76	1,00	−0,46
A.S.	−0,08	0,74	−0,55	−0,38	0,38	−0,06	0,59	−0,59	−0,72	0,75	−0,46	1,00

b1)

Shoreline	Nr_MPs	C.	W.	O.	T.	Area (μm^2)	A.	S.A.	S.R.	R.	Reg	P.I	I.	A.S.
Nr_MPs	1,00	−0,70	0,57	0,50	−0,50	0,29	−0,32	0,50	0,13	0,38	−0,68	0,31	0,64	−0,45
C.	−0,70	1,00	−0,70	−0,79	0,79	−0,09	0,40	−0,27	−0,43	−0,44	0,80	−0,35	−0,81	0,55
W.	0,57	−0,70	1,00	0,51	−0,51	−0,06	−0,45	0,66	0,07	0,54	−0,51	0,61	0,50	−0,57
O.	0,50	−0,79	0,51	1,00	−1,00	−0,04	−0,54	0,15	0,72	0,35	−0,74	0,41	0,72	−0,61
T.	−0,50	0,79	−0,51	−1,00	1,00	0,04	0,54	−0,15	−0,72	−0,35	0,74	−0,41	−0,72	0,61
Area (μm^2)	0,29	−0,09	−0,06	−0,04	0,04	1,00	0,34	0,06	−0,27	0,11	−0,21	−0,32	0,34	0,02
A.	−0,32	0,40	−0,45	−0,54	0,54	0,34	1,00	−0,57	−0,63	−0,44	0,45	−0,76	−0,37	0,55
S.A.	0,50	−0,27	0,66	0,15	−0,15	0,06	−0,57	1,00	−0,17	0,50	−0,29	0,72	0,27	−0,42
S.R.	0,13	−0,43	0,07	0,72	−0,72	−0,27	−0,63	−0,17	1,00	0,13	−0,46	0,30	0,40	−0,40
R.	0,38	−0,44	0,54	0,35	−0,35	0,11	−0,44	0,50	0,13	1,00	−0,35	0,41	0,42	−0,46
Reg	−0,68	0,80	−0,51	−0,74	0,74	−0,21	0,45	−0,29	−0,46	−0,35	1,00	−0,34	−0,90	0,77
P.I	0,31	−0,35	0,61	0,41	−0,41	−0,32	−0,76	0,72	0,30	0,41	−0,34	1,00	0,14	−0,55
I.	0,64	−0,81	0,50	0,72	−0,72	0,34	−0,37	0,27	0,40	0,42	−0,90	0,14	1,00	−0,64
A.S.	−0,45	0,55	−0,57	−0,61	0,61	0,02	0,55	−0,42	−0,40	−0,46	0,77	−0,55	−0,64	1,00

b2)

Berm	Nr_MPs	C.	W.	O.	T.	Area (μm^2)	A.	S.A.	S.R.	R.	Reg	P.I	I.	A.S.
Nr_MPs	1,00	−0,81	0,19	0,19	−0,19	−0,24	0,47	0,19	−0,42	0,56	0,06	0,46	−0,65	−0,53
C.	−0,81	1,00	−0,15	−0,22	0,22	0,18	−0,38	−0,34	0,49	−0,74	0,32	−0,57	0,46	0,54
W.	0,19	−0,15	1,00	0,81	−0,81	−0,15	0,29	0,81	−0,56	0,14	−0,35	0,60	−0,40	−0,48
O.	0,19	−0,22	0,81	1,00	−1,00	−0,04	0,49	0,82	−0,69	0,17	−0,32	0,55	−0,44	−0,40
T.	−0,19	0,22	−0,81	−1,00	1,00	0,04	−0,49	−0,82	0,69	−0,17	0,32	−0,55	0,44	0,40
Area (μm^2)	−0,24	0,18	−0,15	−0,04	0,04	1,00	−0,04	−0,12	0,05	0,06	−0,01	−0,10	0,12	−0,06
A.	0,47	−0,38	0,29	0,49	−0,49	−0,04	1,00	0,34	−0,72	0,27	0,13	0,16	−0,35	−0,26
S.A.	0,19	−0,34	0,81	0,82	−0,82	−0,12	0,34	1,00	−0,81	0,35	−0,44	0,46	−0,23	−0,42
S.R.	−0,42	0,49	−0,56	−0,69	0,69	0,05	−0,72	−0,81	1,00	−0,53	0,23	−0,30	0,23	0,39
R.	0,56	−0,74	0,14	0,17	−0,17	0,06	0,27	0,35	−0,53	1,00	−0,24	0,47	−0,38	−0,50
Reg	0,06	0,32	−0,35	−0,32	0,32	−0,01	0,13	−0,44	0,23	−0,24	1,00	−0,47	−0,25	0,22
P.I	0,46	−0,57	0,60	0,55	−0,55	−0,10	0,16	0,46	−0,30	0,47	−0,47	1,00	−0,70	−0,55
I.	−0,65	0,46	−0,40	−0,44	0,44	0,12	−0,35	−0,23	0,23	−0,38	−0,25	−0,70	1,00	0,45
A.S.	−0,53	0,54	−0,48	−0,40	0,40	−0,06	−0,26	−0,42	0,39	−0,50	0,22	−0,55	0,45	1,00

depending on the number of MPs present. Before proceeding with the counting, a training period of approximately one week was conducted to refine the technique. Each sample was counted three times by three different operators. Given the short analysis times (approximately 2 h for each sample), there is a lower probability of sample contamination, if the right precautions are taken, such as using a clean controlled room without windows, having an air-conditioning system with air filters, and sterile cotton lab coats for the operators. This method allows for the manual separation of microparticles and their preservation in specific sterile supports, enabling subsequent analyses and treatments on the samples. For instance, we prepared the samples for SEM-EDS analysis and Micro-Raman analysis. If necessary, the collected microparticles can

undergo digestive processes to remove the organic substance covering them, which often causes fluorescence during data acquisition in Raman Microscopy (see below).

Given the environment in which they are found, our MPs and MFs have certainly undergone alteration processes (as indicated by the OM, SEM-EDS, and Micro Raman analyses). Additionally, analyses of the YI (%) on manually isolated particles, according to Abaroa-Pérez et al., [33], could be performed to obtain more information on their degree of alteration. Based on the researchers' needs, without conducting spectroscopic analyses, the method described in Peiponen et al. [31] could be followed, as proposed in Fig. 2.

Our protocol includes a comprehensive morphological characterization of MPs and MFs, allowing for useful correlations to understand the accumulation and degradation processes of these microparticles. For example, the protocol described in Goyetche et al. [14] focuses solely on recognizing and characterizing the shape, size, and polymeric composition of MPs. However, the chemical classification and identification of microplastics, which rely on reference spectra of pure polymers, may be compromised because environmental microplastics may contain chemical additives, may accumulate biofilms on their surfaces, and undergo chemical/physical degradation processes. Additionally, the presence of inorganic sediment fragments on the surface of microplastics, their irregular surfaces, and the small size of MPs affect an accurate classification. Finally, regarding the characterization of beach sediments, two aspects of the samples we studied could significantly complicate the implementation of the Goyetche et al., [14] protocol, in our case study: a) the complex mineralogical composition of sediments, including feldspars, clinopyroxenes, leucite, olivine, biotite, nepheline, garnet, amphiboles, quartz, carbonates (calcite, dolomite), and iron and titanium oxides [65]; b) a high and variable spatial heterogeneity in the mineralogical composition of sediments from different beaches [65].

The protocol described in Ferrante et al. [25], like ours, involves the use of a minimal sample quantity for extracting polymeric microparticles with a density greater than 1 g/cm^3 from various environmental matrices, including sediments. This protocol includes a pretreatment of the sample using nitric acid, dichloromethane, and acetonitrile, as well as centrifugation. Applying this protocol to our samples would cause chemical and physical damage to MPs and especially MFs [26], which are highly prevalent in our marine sediments. This would lead to a completely incorrect interpretation of the morphology of MPs, the sizes of MPs and MFs, and the degree of alteration of MPs e MFs. All these parameters have been crucial for reconstructing the depositional dynamics of the microparticles.

Regarding the morphological characterization of MPs alone, we found a favorable comparison in Ocampo et al. [32] despite their protocol involving pretreatment (separation and washing), which requires MPs to be cleaned and separated for applicability. For our study, it is essential to unify the protocols already present in the literature for describing MPs and MFs. To achieve this goal, we have adapted certain parts of Ocampo et al.'s method to fit our needs, using terminology related to the description of shape and the degree of surface roughness and smoothness (degree of alteration), specifically focusing on MPs. Their protocol relies on advanced image data management software and geometric function interpretation. However, this approach is impractical if one opts not to proceed with pretreatments because environmental matrices, whether organic or inorganic, consistently interact with MPs, adhering to them and altering their perimeter and surface. In our case, image data is scrutinized, managed, and interpreted by an operator proficient in recognizing both organic particles (such as algae fragments, wood debris, microorganisms, etc.) and inorganic particles (rock fragments, minerals, and glass).

3.3. Detailed morphological and qualitative chemical analysis

Chemical EDS analyses correlated with morphological analyses indicating the presence of sediment microcrystals, both on the surface and in the folds of flat morphology microfibers. The analyses of sediment fragments on MFs surface show the presence of ferromagnesian minerals, calcium silicates, sodium, and potassium (Fig. 7A) attributable to that of the typical rocks of the Vesuvian area such as plagioclase and feldspars, clinopyroxene, Fe oxides, micas, etc.

In some cases, the presence of P, Si, Ca, Na, Cl, O, and C has been found (Fig. 7B), attributable to organic matter such as phosphates, organisms with siliceous shells, and halite; there are no heavy metals. EDS analyses were performed on MFs, and a different chemical composition was found based on morphology. Based on Wang et al. [48], the qualitative analyses carried out by EDS associated with morphological analyses (SEM) can give information on the polymers that make up the MPs. In our study, the round MFs (Fig. 7D) show, in most cases, only C in the EDS spectrum, therefore it could be polypropylene (PP), polyethylene (PE), or polystyrene (PS). Oxygen can be due to both the polymers such as Nylon (PA) or PET, or to degradation processes as reported [46,48]. This finding is in line with the studies carried out by [66], Corpas et al. [44], and Fateminia et al. [67], on the morphology of PP, PE, and PA fibers confirmed also of MicroRaman analyses. For flat MFs the EDS spectra collected, in most cases, show the presence of C, and Cl (Fig. 7C) and could therefore be PVC [48]. Again, based on Pham et al. [47], we study the morphology of PVC, and we can confirm that the flat MFs are made of PVC. In other cases, however, the flat MFs have a chemical composition characterized only by the presence of C; in this case, they could be made of polyethylene (PE; [50]). Mahltig and Grethe [46] characterize the PPS fibers with SEM-EDS analyses, well correlating with the data collected for some microfibers found in our samples, composed by C and S. Zhong et al. [68] characterized the PVEA polymer with SEM-EDS data well correlating with the morphological and qualitative data collected for some MFs opaque (Fig. 7E). Although less frequently, for the opaque flat and cylindrical MFs with a high degree of alteration, in OM we identified natural fibers, such as wool or cotton (cellulose). The morphological analyses of detail at SEM, have confirmed the presence of natural fibers such as wool and cotton that present a strong degree of alteration.

Raman spectra were registered to identify the chemical nature of the MFs collected at SGa-S, SGa-BE, SGb-BE, PO-S, PO-BE, and ER-BE sites. The analysis of the spectra revealed that 12 out of 30 samples are fluorescent at the laser line used for the measurement (514 nm). This phenomenon hampers the identification of the Raman features of the sample. The remaining 18 MFs provided Raman spectra that allowed us to identify the chemical nature of the materials under investigation (Table 4). A sample collected at the SGa_BE site showed unambiguous features compatible with polystyrene (PS). Polyamide (PA/Nylon) was identified in the SGa_S site, polyacrylonitrile (PAN) in SGb_BE, and polyethylene terephthalate (PET) in PO_BE and SGa_BE sites. All the other samples showed features compatible with dyed cotton fibers (both grey/white or indigo). Representative Raman spectra and the quantitative distribution of the identified MF samples are reported in Fig. S3 and Fig. 8, respectively. In summary, the Raman analyses conducted on 30 untreated MFs revealed that 40 % of the samples are fluorescent, and it was not possible to identify the nature of these particles, probably due to the presence of organic substances and/or specific types of dyes on their surface. The remaining 60 % consists of synthetic (PA, PAN, PET, and PS) and cotton-based fibers. The relative occurrence of synthetic MFs versus the natural ones identified is around 1:2.5. Raman analyses were also performed on 7 MP samples collected at ER_BE, PO_BE, SGa_BE, and SGa_S sites. However, all of them were fluorescent. In some cases, a signal (1086 cm^{-1}) attributable to calcite was detected (data not shown), probably due to the presence of some surface encrustation. All the fluorescent MF or MP samples could correspond to additional polymer species, as those suggested via SEM (PE, PP, PVC, and PVEA). Most likely the use of a NIR laser source might decrease the count on fluorescent samples.

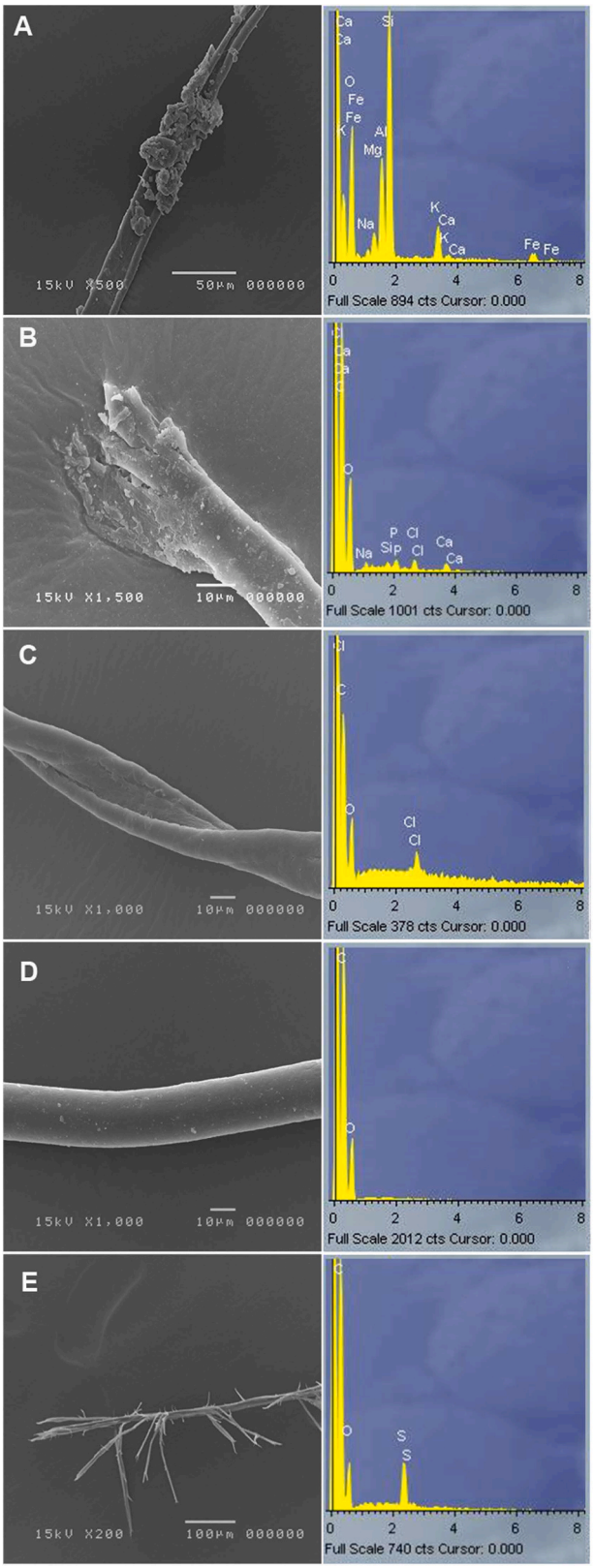

Fig. 7. SEM images and EDS spectra. **A** The spectrum indicates the chemical composition of sediments microparticles trapped in flat MFs. **B** The spectrum indicates the presence of organic materials on round MFs surface. **C.** The spectrum shows the polymeric composition of the flat MFs, characterized by the presence of C and Cl. **D**. Chemical composition of the round MFs, characterized by the presence of C. **E**. Polymeric composition of the MFs with flat arborescent morphology, characterized by the presence of C and S.

Table 4
Identification of the MFs by Raman analysis.

Site ID	Sample ID	Raman assignment	Sample shape
SGa-S	1	Polyamide (PA/Nylon)	Round
	2	Indigo dyed cotton fiber	Round
SGa-BE	3	Polystyrene (PS)	Round
	4, 5, 6	Grey/white dyed cotton fiber	Flat
	7	Polyethylene terephthalate (PET)	Round
SGb-BE	8, 9	Indigo dyed cotton fiber	Round
	10	Polyacrylonitrile (PAN)	Flat
PO-BE	11	Grey/white dyed cotton fiber	Round
	12, 13	Grey/white dyed cotton fiber	Flat
	14	Polyethylene terephthalate (PET)	Round
ER-BE	15	Grey/white dyed cotton fiber	Round
	16, 17	Indigo dyed cotton fiber	Round
	18	Grey/white dyed cotton fiber	Flat

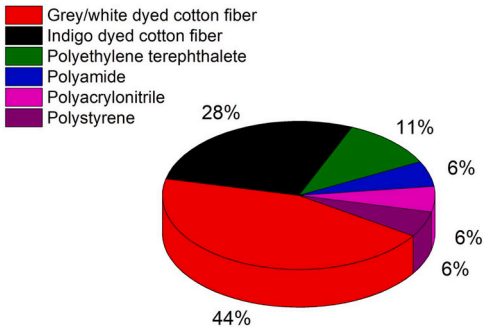

Fig. 8. Quantitative distribution of the MF samples identified by Raman analysis.

4. Conclusions

This work highlights how it is possible to analyze MPs and MFs present in sediments without pretreatments based on observation under optical microscopy. Observation can also be carried out on minimal sediment quantities of 1.5 g without losing and/or distorting important information (number, length, degree of alteration, presence of organic matter, etc.). Furthermore, depending on the needs of the researchers', characterization can be performed either live, proceeding simultaneously with the separation of MPs and MFs, or remotely (using previously collected image data). The method allows researchers to conduct further investigations on manually separated microparticles, such as SEM-EDS and MicroRaman, as in our case, as well as NIR-HIS, Py-GC-MS, and Micro FT-IR. Pretreatments such as digestion can also be included, depending on the researchers' need to explore various aspects of MPs and MFs. This protocol has some disadvantages: a) the researcher using the protocol must have extensive experience not only in recognizing and describing MPs and MFs, but also in identifying all elements that compose the matrix in which they are found, as organic product, algae, echinoids spicules, rocks, minerals fragments, etc.; b) the high quality of the stereomicroscope optics is not available in all laboratories.

This method allows for understanding the accumulation processes of MPs and MFs, immediately highlighting anomalies corresponding to specific coastal accumulation processes and/or morphological information of sampling sites (foreshore, berm, etc.). Furthermore, it can provide crucial insights into pollutant sources, thus enabling timely intervention to address sensitive environmental issues.

We believe that this protocol can also be applied to other environmental matrices; experiments on soil, compost, and colony of unicellular algae are underway.

Environmental Implication

The presence of microplastics in aquatic environments, including

marine sediments, poses an environmental hazard. Once released into the environment, microplastics can be ingested by biota and accumulate in organisms. Monitoring the presence of microplastic is crucial. Protocols for studying microplastics in marine sediments involve density separation and digestion processes but have gaps such as the use of toxic substances. Our protocol, based on optical microscopy, is eco-friendly, rapid, and requires no pretreatment. It has allowed us to identify the dynamics of microplastic accumulation and pollution sources on the beaches of the Vesuvian coast, an area heavily impacted by human activity.

CRediT authorship contribution statement

Mariarca D'Aniello: Visualization, Data curation. **Manuela Rossi:** Writing – review & editing, Writing – original draft, Supervision, Software, Project administration, Methodology, Investigation, Formal analysis, Data curation, Conceptualization. **Carlo Donadio:** Writing – review & editing, Writing – original draft, Validation, Supervision, Methodology, Investigation, Conceptualization. **Alessandro Vergara:** Writing – review & editing, Writing – original draft, Supervision, Investigation, Formal analysis, Data curation. **Fiore Capozzi:** Writing – review & editing, Writing – original draft, Supervision, Data curation. **Simonetta Giordano:** Validation, Supervision, Data curation, Conceptualization. **Noemi Fiaschini:** Visualization, Investigation. **Tonia Tommasi:** Writing – review & editing, Validation, Supervision. **Marco Guida:** Writing – review & editing, Visualization. **Valeria Spagnuolo:** Validation, Supervision. **Romualdo Troisi:** Writing – original draft, Investigation, Formal analysis. **Vincenzo Vedi:** Investigation, Formal analysis, Data curation. **Filippo Ambrosi de Magistris:** Software, Investigation.

Declaration of Competing Interest

The authors declare that they have no known competing financial interests or personal relationships that could have appeared to influence the work reported in this paper.

Data Availability

Data will be made available on request.

Appendix A. Supporting information

Supplementary data associated with this article can be found in the online version at doi:10.1016/j.jhazmat.2024.135272.

References

[1] Arthur, C., Baker, J., 2012. Proceedings of the second research workshop on microplastic marine debris. NOAA marine debris program, U.S. department of commerce, silver spring, MD: national oceanic and atmospheric administration, technical memorandum NOS-OR&R-39. Univ Wash Tacoma, Tacoma, WA, USA 9–11.

[2] Arthur, C., Bamford, H., Baker, J., 2009. Proceedings of the international research workshop on the occurrence, effects, and fate of microplastic marine debris. NOAA marine debris program, national oceanic and atmospheric administration, U.S. department of commerce, technical memorandum NOS-OR&R-30. Univ Wash Tacoma, Tacoma, WA, USA 528p..

[3] Browne, M.A., Galloway, T., Thompson, R., 2007. Microplastic an emerging contaminant of potential concern? Integr Environ Assess Manag 3 (4), 559–561. https://doi.org/10.1002/ieam.5630030412.

[4] Masura, J., Baker, J., Foster, G., Arthur, C., Herring, C., 2015. Laboratory methods for the analysis of microplastics in the marine environment: recommendations for quantifying synthetic particles in waters and sediments. 1. NOAA marine debris program. Natl Ocean Atmos Adm US Dep Commer 31p.

[5] Harrison, J.P., Sapp, M., Schratzberger, M., Osborn, A.M., 2011. Interactions between microorganisms and marine microplastics: a call for research. Mar Technol Soc J 45, 12–20. https://doi.org/10.4031/MTSJ.45.2.2.

[6] Kershaw, P., 2015. Sources, fate and effects of microplasticsin the marine environment: a global assessment. GESAMP Fr. https://doi.org/10.13140/RG.2.1.3803.7925.

[7] Kershaw, P.J., and Chelsea, M.R. (2016). "Sources, Fate and Effects of Microplastics in the Marine Environment: Part 2 of a Global Assessment." Reports and Studies 93, 220 pp. - IMO/FAO/UNESCO-IOC/WMO/IAEA/UN/UNEP Joint Group of Experts on the Scientific Aspects of Marine Environmental Protection (GESAMP).

[8] Lusher, A.L., Bråte, I.L.N., Munno, K., Hurley, R.R., Welden, N.A., 2020. Is it or isn't it: the importance of visual classification in microplastic characterization. Appl Spectrosc 74 (9). https://doi.org/10.1177/0003702820930733.

[9] Royer, S., Wiggin, K., Kogler, M., Deheyn, D.D., 2021. Degradation of synthetic and wood-based cellulose fabrics in the marine environment: Comparative assessment of field, aquarium, and bioreactor experiments. Sci Total Environ 791, 148060. https://doi.org/10.1016/j.scitotenv.2021.148060.

[10] Arienzo, M., Donadio, C., 2023. Microplastic–pharmaceuticals interaction in water systems. J Mar Sci Eng 11, 1437. https://doi.org/10.3390/jmse11071437.

[11] Wright, S.L., Thompson, R.C., Galloway, T.S., 2013. The physical impacts of microplastics on marine organisms: a review. Environ Pollut 178, 483–492. https://doi.org/10.1016/j.envpol.2013.02.031.

[12] Suaria, G., Aikaterini, A., Perold, V., Lee, J.R., Pierucci, A., Bornman, T.G., Aliani, S., Ryan, P.G., 2020. Microfibers in oceanic surface waters: a global characterization. Sci Adv 6 (23), eaay8493. ⟨https://www.science.org/doi/10.1126/sciadv.aay8493⟩.

[13] Fu, W., Min, J., Jiang, W., Li, Y., Zhang, W., 2020. Separation, characterization and identification of microplastics and nanoplastics in the environment. Sci Total Environ 721, 137561. https://doi.org/10.1016/j.scitotenv.2020.137561.

[14] Goyetche, R., Kortazar, L., and Amigo, J.M. Issues with the detection and classification of microplastics in marine sediments with chemical imaging and machine learning. Trends in Analytical Chemistry. 117221. https://doi.org/10.1016/j.trac.2023.117221.

[15] Zhao, K., Wei, Y., Dong, J., Zhao, P., Wang, Y., Pan, X., Wang, J., 2022. Separation and characterization of microplastic and nanoplastic particles in marine environment. Environ Pollut 297, 118773. https://doi.org/10.1016/j.envpol.2021.118773.

[16] Cashman, M.A., Ho, K.T., Boving, T.B., Russo, S., Robinson, S., Burgess, R.M., 2020. Comparison of microplastic isolation and extraction procedures from marine sediments. Mar Pollut Bull 159, 111507. https://doi.org/10.1016/j.marpolbul.2020.111507.

[17] Hurley, R., Woodward, J., Rothwell, J.J., 2018. Microplastic contamination of river beds significantly reduced by catchment-wide flooding. Nat Geosci 11 (4), 251–257. https://doi.org/10.1038/s41561-018-0080-1.

[18] Nuelle, M.T., Dekiff, J.H., Remy, D., Fries, E., 2014. A new analytical approach for monitoring microplastics in marine sediments. Environ Pollut 184, 161–169. https://doi.org/10.1016/j.envpol.2013.07.027.

[19] Phuong, N.N., Fauvelle, V., Grenz, C., Ourgaud, M., Natascha Schmidt, N., Strady, E., Sempéré, R., 2021. Highlights from a review of microplastics in marine sediments. Sci Total Environ 777, 146225. https://doi.org/10.1016/j.scitotenv.2021.146225.

[20] Singh, S., Kumar, Naik, T.S.S., Anil, A.G., Dhiman, J., Kumar, V., Dhanjal, D.S., Aguilar-Marcelino, L., Singh, J., Ramamurthy, P.C., 2022. Micro (nano) plastics in wastewater: a critical review on toxicity risk assessment, behaviour, environmental impact and challenges. Chemosphere 290, 133169. https://doi.org/10.1016/j.chemosphere.2021.133169.

[21] Zobkov, M.B., Esiukova, E.E., 2018. Microplastics in a marine environment: review of methods for sampling, processing, and analyzing microplastics in water, bottom sediments, and coastal deposits. Oceanology 58 (1), 137–143. https://doi.org/10.1134/S0001437017060169.

[22] Asakura, H., 2023. Accuracy of a simple microplastics investigation method on sandy beaches. Microplastics 2 (3), 304–321. https://doi.org/10.3390/microplastics2030024.

[23] Culligan, N., Liu, K.-b, Ribble, K., Ryu, J., Dietz, M., 2022. Sedimentary records of microplastic pollution from coastal Louisiana and their environmental implications. J Coast Conserv 26 (1). https://doi.org/10.1007/s11852-021-00847-y.

[24] Ronda Ana, C., Arias Andrés, H., Oliva Ana, L., Marcovecchio, J.E., 2019. Synthetic microfibers in marine sediments and surface seawater from the Argentinean continental shelf and a Marine Protected Area. Mar Pollut Bull 149, 110618. https://doi.org/10.1016/j.marpolbul.2019.110618.

[25] Ferrante, M., Oliveri Conti, G., Zuccarello, P., 2020. Patent method for the extraction and determination of micro-and nano-plastics in organic and inorganic matrix samples: An application on vegetals. MethodsX 7, 100989 https://doi.org/10.1016/j.mex.2020.100989Get rights and content.

[26] Li, P., Lai, Y., Zheng, R.G., Li, Q.C., Sheng, X., Yu, S., Hao, Z., Cai, Y.Q., Liu, J., 2023. Extraction of common small microplastics and nanoplastics embedded in environmental solid matrices by tetramethylammonium hydroxide digestion and dichloromethane dissolution for Py-GC-MS determination. Environ Sci Technol 57 (32), 12010–12018. https://doi.org/10.1021/acs.est.3c03255.

[27] Frias, J., Pagter, E., Nash, R., O'Connor, I., Carretero, O., Filgueiras, A., Viñas, L., Gago, J., Antunes, J., Bessa, F., Sobral, P., Goruppi, A., Tirelli, V., Pedrotti, M.L., Suaria, G., Aliani, S., Lopes, C., Raimundo, J., Caetano, M., Gerdts, G., 2018. Standardized protocol for monitoring microplastics in sediments. JPI Oceans Baseman Micro Anal Eur Waters Deliv D4 2. ⟨http://www.jpi-oceans.eu/baseman/main-page⟩.

[28] Harris, P.T., 2020. The fate of microplastic in marine sedimentary environments: a review and synthesis. Mar Pollut Bull 158, 111398. https://doi.org/10.1016/j.marpolbul.2020.111398.

[29] Valente, T., Ventura, D., Matiddi, M., Sbrana, A., Silvestri, C., Piermarini, R., Jacomini, C., Costantini, M.L., 2023. Image processing tools in the study of environmental contamination by microplastics: reliability and perspectives.

Environ Sci Pollut Res 30, 298–309. https://doi.org/10.1007/s11356-022-22128-3.
[30] Yu, J.T., Helm, P.A., Diamond, M.L., 2024. Source-specific categorization of microplastics in nearshore surface waters of the Great Lakes. J Gt Lakes Res 50 (1), 102256. https://doi.org/10.1016/j.jglr.2023.102256.
[31] Peiponen, K.E., Kanyathare, B., Hrovat, B., Papamatthaiakis, N., Hattuniemi, J., Asamoah, B., Haapala, A., Koistinen, A., Roussey, M., 2023. Sorting microplastics from other materials in water samples by ultra-high-definition imaging. J Eur Opt Soc-Rapid Publ 19 (1), 14. https://doi.org/10.1051/jeos/2023010.
[32] Ocampo, G.O.D., Goizueta, J.I., Lavarello, F., Churio, M.S., Mendive, C.B., 2024. Facile, inexpensive, and reliable morphological characterization of microplastics using optical microscopy images. Chem Phys 583, 112326. https://doi.org/10.1016/j.chemphys.2024.112326.
[33] Abaroa-Pérez, B., Ortiz-Montosa, S., Hernández-Brito, J.J., Vega-Moreno, D., 2022. Yellowing, weathering and degradation of marine pellets and their influence on the adsorption of chemical pollutants. Polym (Basel) 14 (7), 1305. https://doi.org/10.3390/polym14071305.
[34] Barrows, A.P.W., Cathey, S.E., Petersen, C.W., 2018. Marine environment microfiber contamination: global patterns and the diversity of microparticle origins. Environ Pollut 237, 275–284. https://doi.org/10.1016/j.envpol.2018.02.062.
[35] Gniadek, M., Dąbrowska, A., 2019. The marine nano- and microplastics characterization by SEM EDX: the potential of the method in comparison with various physical and chemical approaches. Mar Pollut Bull 148, 210–216. https://doi.org/10.1016/j.marpolbul.2019.07.067.
[36] Delogu, M.R., D'Aniello, M., Giovanzanti, A., Guadagno, E., Lemmle, L., Perez, Filho, A., Perriello, Zampelli, S., Sannino, S., Valente, R., Donadio, C., 2023. Environmental and geomorphic aspects of urban beaches of Naples, southern Italy. BORNH 3 (3), 24–45. https://doi.org/10.6093/2724-4393/10811.
[37] Arienzo, M., Bolinesi, F., Aiello, G., Barra, D., Donadio, C., Stanislao, C., Ferrara, L., Mangoni, O., Toscanesi, M., Giarra, A., Trifuoggi, M., 2020. The environmental assessment of an estuarine transitional environment, southern Italy. J Mar Sci Eng 8 (9), 628. https://doi.org/10.3390/jmse8090628.
[38] Bui, E.N., Mazullo, J., Wilding, L.P., 1990. Using quartz grain size and shape analysis to distinguish between aeolian and fluvial deposits in the Dallol Bosso of Niger (West Africa). Earth Surf Process Landf 14, 157–166. https://doi.org/10.1002/esp.3290140206.
[39] Pennetta, M., Stanislao, C., D'Ambrosio, V., Marchese, F., Minopoli, C., Trocciola, A., Valente, R., Donadio, C., 2018. Geomorphological features of the archaeological marine area of Sinuessa in Campania, southern Italy. Quat Int 425, 198–213. https://doi.org/10.1016/j.quaint.2018.06.041.
[40] Blott, S.J., Pye, K., 2001. GRADISTAT: a particle size distribution and statistics package for the analysis of unconsolidated sediments. Earth Surf Process Landf 26, 1237–1248. https://doi.org/10.1002/esp.261.
[41] Folk, R.L., Ward, W.C., 1957. Brazos River bar: a study in the significance of grain size parameters. J Sediment Petrol 27, 3–26.
[42] Graham, D., Midgley, N.G., 2000. Graphical representation of particle shape using triangular diagrams: an excel spreadsheet method. Earth Surf Process Landf 25, 1473–1477 https://doi.org/10.1002/1096-9837(200012)25:13<1473: AID-ESP158>3.0.CO;2-C.
[43] Liu, J., Liu, Q., An, L., Wang, M., Yang, Q., Zhu, B., Ding, J., Ye, C., Xu, Y., 2022. Microfiber pollution in the earth system. Rev Environ Contam Toxicol 260 (1), 13. https://doi.org/10.1007/s44169-022-00015-9.
[44] Corpas, F.A., González, B., Gómez, L., Rosa, F., Figueroa, J.M., 2013. The fire resistence of concrete with polypropylene fibers. MATEC Web Conf 6, 02005. https://doi.org/10.1051/matecconf/20130602005.
[45] He, Z., Nam, S., Fang, D.D., Cheng, H.N., He, J., 2021. Surface and of phenotypes differing in fiber. Polymers 13 (7), 994. https://doi.org/10.3390/polym13070994.
[46] Mahltig, B., Grethe, T., 2022. High-performance and functional fiber materials—a review of properties, SEM and EDS. Textiles 2 (2), 209–251. https://doi.org/10.3390/textiles2020012.
[47] Pham, T.H., Do, H.T., Thi, L.A.P., Singh, P., Raizada, P., Wu, J.C.S., Nguyen, V.H., 2021. Global challenges in microplastics: From fundamental understanding to advanced degradations toward sustainable strategies. Chemosphere 267, 129275. https://doi.org/10.1016/j.chemosphere.2020.129275.
[48] Wang, Z.-M., Wagner, J., Ghosal, S., Bedi, G., Wall, S., 2017. SEM/EDS and optical microscopy analyses of microplastics in ocean trawl and fish guts. Sci Total Environ 603-604, 616–626. https://doi.org/10.1016/j.scitotenv.2017.06.047.
[49] Zhou, Q., Zhang, H., Fu, C., Zhou, Y., Dai, Z., Li, Y., Tu, C., Luo, Y., 2018. The distribution and morphology of microplastics in coastal soils adjacent to the Bohai Sea and the Yellow Sea. Geoderma 322, 201–208. https://doi.org/10.1016/j.geoderma.2018.02.015.
[50] Zhu, B., Liu, J., Wang, T., Han, M., Valloppilly, S., Xu, S., Wang, X., 2017. Novel polyethylene fibers of very high thermal conductivity enabled by amorphous restructuring. ACS Omega 2 (7), 3931–3944. https://doi.org/10.1021/acsomega.7b00563.
[51] Oxford Instruments (2006): INCA - The microanalysis suite issue 17a C SP1 – Version 4.08. Oxford Instr. Anal. Ltd., Oxfordshire, United Kingdom.
[52] Absher, T.M., Ferreira, S.L., Kern, Y., Ferreira, A.L.Jr, Christo, S.W., Ando, R.A., 2019. Incidence and identification of microfibers in ocean waters in Admiralty Bay, Antarctica. Environ Sci Pollut Res 26 (1), 292–298. https://doi.org/10.1007/s11356-018-3509-6.
[53] Athey, S.N., Erdle, L.M., 2022. Are we underestimating anthropogenic microfiber pollution? A critical review of occurrence, methods, and reporting. Environ Toxicol Chem 41 (4), 822–837. https://doi.org/10.1002/etc.5173.
[54] Jones, N.R., de Jersey, A.M., Lavers, J.L., Rodemann, T., Rivers-Auty, J., 2024. Identifying laboratory sources of microplastic and nanoplastic contamination from the air, water, and consumables. J Hazard Mater 465, 133276. https://doi.org/10.1016/j.jhazmat.2023.133276.
[55] Anger, P.M., Von der Esch, E., Baumann, T., Elsner, M., Niessner, R., Ivleva, N.P., 2018. Raman microspectroscopy as a tool for microplastic particle analysis. Trends Anal Chem 109, 214–226. https://doi.org/10.1016/j.trac.2018.10.010.
[56] Capozzi, F., Sorrentino, M.C., Granata, A., Vergara, A., Alberico, M., Rossi, M., Spagnuolo, V., Giordano, S., 2023. Optimizing moss and lichen transplants as biomonitors of airborne anthropogenic microfibers. Biology 12 (10), 1278. https://doi.org/10.3390/biology12101278.
[57] Karapanayiotis, T., Villar, S.E.J., Bowen, R.D., Edwards, H.G., 2004. Raman spectroscopic and structural studies of indigo and its four 6,60-dihalogeno analogues. Analyst 129 (7), 613–618. https://doi.org/10.1039/b401798f.
[58] Zapata, F., Ortega-Ojeda, F.E., García-Ruiz, C., 2022. Forensic examination of textile fibres using Raman imaging and multivariate analysis. Spectrochim Acta Part A, Mol Biomol Spectrosc 268, 120695. https://doi.org/10.1016/j.saa.2021.120695.
[59] Avio, C.G., Gorbi, S., Regoli, F., 2017. Plastics and microplastics in the oceans: from emerging pollutants to emerged threat. Mar Environ Res 128, 2–11. https://doi.org/10.1016/j.marenvres.2016.05.012.
[60] Baudena, A., Ser-Giacomi, E., Jalón-Rojas, I., Galgani, F., Pedrotti, M.L., 2022. The streaming of plastic in the Mediterranean Sea. Nat Commun 13, 2981. https://doi.org/10.1038/s41467-022-30572-5.
[61] Kaandorp, M.L.A., Lobelle, D., Kehl, C., Dijkstra, H.A., van Sebille, E., 2023. Global mass of buoyant marine plastics dominated by large long-lived debris. Nat Geosci 16, 689–694. https://doi.org/10.1038/s41561-023-01216-0.
[62] Pradan, U., Naik, S., Begum, M., Kumar, S.S., Panda, U.S., Mishra, P., Murthy, M.V. R., 2018. Marine litter: post-flood nuisance for Chennai beaches. Sci Corres Curr Sci 115 (8), 1454–1455. https://doi.org/10.18520/cs%2Fv115%2Fi8%2F1454-1455.
[63] Van Cauwenberghe, L., Devriese, L., Galgani, F., Robbens, J., Janssen, C.R., 2015. Microplastics in sediments: a review of techniques, occurrence and Effects. Mar Environ Res 111, 5–17. https://doi.org/10.1016/j.marenvres.2015.06.007.
[64] Van Emmerik, T., Strady, E., Kieu-Le, T.-C., Nguyen, L., Gratiot, N., 2019. Seasonality of riverine macroplastic transport. Sci Rep 9, 13549. https://doi.org/10.1038/s41598-019-50096-1.
[65] Morrone, C., Le Pera, E., Marsaglia, K.M., De Rosa, R., 2019. Compositional and textural study of modern beach sands in the active volcanic area of the Campania region (southern Italy). Sediment Geol 396, 105567. https://doi.org/10.1016/j.sedgeo.2019.105567.
[66] Qiang, L., Cheng, J., 2019. Exposure to microplastics decreases swimming competence in larval zebrafish (Danio rerio). Ecotoxicol Environ Saf 176, 226–233. https://doi.org/10.1016/j.ecoenv.2019.03.088.
[67] Fateminia, Z., Chiniforoshan, H., Vahid, Ghafarinia, V., 2023. Novel core/shell nylon 6,6/La-TMA MOF electrospun nanocomposite membrane and CO_2 capture assessments of the membrane and Pure La-TMA MOF. ACS Omega 8 (25), 22742–22751.
[68] Zhong, C., Jiang, L., Peng, X., 2010. Synthesis and solution behavior of comb-like terpolymers with polyethylene oxide macromonomer. J Polym Sci: Part A: Polym Chem. https://doi.org/10.1002/pola.23888.